UNIVERSIDADE D
COIMBRA

Andreia Filipa Simões Oliveira

NMR METABONOMICS APPLIED TO SYNAPTOSOMES AND SLICES TO PROFILE METABOLIC ALTERATIONS IN NEURODEGENERATIVE AND NEUROPROTECTIVE MECHANISMS

VOLUME 1

Dissertação no âmbito do Mestrado em Bioquímica orientada pelo Professor Doutor Rodrigo Pinto Santos Antunes Cunha e pelo Professor Doutor Rui de Albuquerque Carvalho, apresentada à Faculdade de Ciências e Tecnologia da Universidade de Coimbra, departamento de Ciências da Vida.

Outubro de 2021

Table of Contents

Agradecimentos

Gostaria de deixar aqui alguns agradecimentos especiais a pessoas que contribuíram das mais variadas formas para que pudesse concluir este projeto e me ajudaram neste processo de aprendizagem.

Aos meus orientadores Professor Doutor Rodrigo Cunha e Professor Doutor Rui Carvalho obrigada por todos os conhecimentos transmitidos, pela disponibilidade de me receberem, e por todo o apoio e ajuda preponderantes.

À Doutora Paula Canas, obrigada por toda a ajuda, todos os conhecimentos e conselhos, pela disponibilidade e preocupação.

A todo o grupo *Purines Lab*, obrigada por me acolherem tão bem, me ajudarem nas diferentes etapas e pelo companheirismo.

À Joana e à Bárbara, muito obrigada pela paciência, por me ouvirem sempre, pelo apoio e pela amizade.

Aos meus amigos, na faculdade e fora, agradeço todos os momentos, gargalhadas e apoio que me prestam nesta etapa da minha vida e nas restantes.

À minha família, em especial aos meus pais e irmão que nunca deixam de acreditar em mim e puxar para cima nos momentos mais complicados. Obrigada por todo o carinho, apoio, disponibilidade e por esta oportunidade.

Por último, a ti João, um obrigado do tamanho do mundo… Pelo amor, carinho, preocupação constante, apoio incondicional e espírito critico. O futuro é nosso.

List of Abbreviations

4 – aminopyridine, 4 AP

4-(2-hydroxyethyl)-1-piperazineethanesulfonic acid, HEPES

A_{2A} receptor knockout, A_{2A}R KO

A_{2A} receptors, A_{2A}Rs

Acetyl coenzyme A, acetyl-CoA

adenosine 5' – monophosphate, AMP

Adenosine triphosphate, ATP

Alzheimer's disease, AD

Amyloid-β protein, Aβ

Bicinchoninic acid assay, BCA

Bovine serum albumin, BSA

Central nervous system, CNS

Ethylenediaminetetraacetic acid, EDTA

Glucose transporter, GLUT

G-protein coupled receptors, GPCR

Lactate dehydrogenase, LDH

Nuclear magnetic resonance, NMR

Oxidative phosphorylation, OXPHOS

Perchloric acid, PCA

Peripheral nervous system, PNS

Phosphofructokinase, PFK

Reactive nitrogen species, RNS

Reactive oxygen species, ROS

Tricarboxylic acid cycle, TCA cycle

Wild – type, WT

γ – aminobutyric acid, GABA

Resumo

Os recetores A_{2A} (A_{2A}Rs) desempenham um papel importante em sinapses de diversas regiões do cérebro, sendo que a sua sobre-ativação provoca défices na plasticidade sináptica e na memória. Sabe-se que o bloqueio dos A_{2A}Rs, seja pela ligação de antagonistas ou pela inativação genética, confere neuroprotecção contra danos cerebrais, nomeadamente nas regiões corticais do cérebro. Por este motivo, estes recetores são apontados como potenciais alvos terapêuticos para diversas doenças neurodegenerativas, como a doença de Alzheimer. Também o metabolismo pode estar intrinsecamente ligado a distúrbios neurodegenerativos, uma vez que estudos indicam que alterações metabólicas influenciam fortemente o início e a progressão de doenças neurodegenerativas.

Muitas doenças associadas ao cérebro começam com disfunção ou perda sináptica, no entanto os mecanismos subjacentes não são totalmente conhecidos. Assim, as alterações metabólicas são propostas como causa possível para a disfunção e perda sináptica. Para além disso, os mecanismos de neuroproteção associados a A_{2A}Rs, como é exemplo a cafeína e a inativação genética dos A_{2A}Rs, não são também totalmente conhecidos, sendo proposto que alterações metabólicas sejam o mecanismo subjacente à neuroproteção.

Para testar esta hipótese de trabalho foram realizadas experiências no modelo animal APP/PS1, que mimetiza a doença de Alzheimer, no modelo A_{2A}R KO, que possui inativação genética dos A_{2A}Rs, e ainda em animais controlo (*wild-type*, WT) sujeitos a tratamento com cafeína. Assim, sinaptossomas P2 e fatias corticais foram utilizados para a realização de estudos metabólicos, efetuados com recurso a espectroscopia de Ressonância Magnética Nuclear (RMN).

Os resultados das experiências realizadas com APP/PS1 mostram que não existem alterações metabólicas significativas em sinaptossomas, estando em concordância com outro estudo que afirma que em vários modelos transgénicos de animais que mimetizam a doença de Alzheimer, não foram observados défices bioenergéticos consistentes em sinaptossomas. Quanto às experiências realizadas nos diferentes mecanismos de neuroproteção, os resultados mostram uma diferença no índice glicolítico entre sinaptossomas e fatias corticais, mas mostram também que não existem alterações significativas nas características metabólicas entre animais controlo e tratados com cafeína, bem como entre animais WT e A_{2A}R KO.

Abstract

A_{2A} receptors (A_{2A}Rs) play a crucial role in controlling synaptic function in multiple brain regions, and their over-activation impairs synaptic plasticity and memory. It is acknowledged that A_{2A}R blockade, using antagonists or genetic inactivation, offers a robust neuroprotection against brain damage, especially in cortical regions of the brain. Hence, several groups have considered A_{2A}Rs as a promising drug target in different pathologies, namely neurodegenerative disorders.

Metabolism is also thought to be intrinsically linked to neurodegenerative disorders as there is increasing evidence suggesting that metabolic alterations strongly influence the onset and progression of neurodegenerative diseases, in accordance with different studies showing that brain disorders are accompanied by specific patterns of cerebral metabolic activity.

Most brain diseases begin with a dysfunction or loss of synapses, though the exact processes involved are still unknown. Nevertheless, metabolic impairments are proposed to underlie synaptic dysfunction and loss. Moreover, neuroprotection mechanisms associated with A_{2A}R, such as caffeine or genetic inactivation of A_{2A}R, also remain undetermined so a link between metabolic alterations or adaptations and neuroprotection is proposed.

To test our working hypothesis, experiments were performed in APP/PS1 mouse model and upon different neuroprotective mechanisms, such as caffeine, and the A_{2A}R KO mouse model, which has a genetic inactivation of A_{2A}R. P2 synaptosomes and superfused cortical slices were used to perform the metabolic experiments with samples being analysed by NMR spectroscopy.

The results show no significant alterations in metabolic features in the cortical synapses of AD-like mice, which is in accordance with another study in several transgenic mouse models of Alzheimer's disease (AD), that reported no consistent bioenergetic deficits. Furthermore, the experiences performed with the neuroprotective mechanisms indicate a difference in glycolytic index between synaptosomes and slices, but there are no significant metabolic alterations between the control group and the group treated with caffeine, and also between WT and A_{2A}R KO mice.

1. Introduction

1.1. Modulation systems in the brain

The nervous system is divided into two parts: (A) the central nervous system (CNS), which consists of the brain and spinal cord; and (B) the peripheral nervous system (PNS), composed of the nerves that connect the brain and spinal cord with the rest of the body. The CNS has several areas, being the cerebral cortex the outer surface, associated with higher level processes such as consciousness, thought, emotion, cognition, and memory (1,2).

The process of receiving and processing information, producing different biological responses is called neurotransmission, in which neurons, electrically active cells, are involved. Neurons communicate through electrical (action potentials) and biochemical (neurotransmitters) signals occurring in synapses (junctions between two neurons) (3). The process of neurotransmission begins when an action potential is generated, causing the pre-synaptic neuron to release neurotransmitters into the synaptic cleft, which will bind to neurotransmitter receptors on the cell membrane of the post-synaptic neuron. Different types of neurotransmitters, for example glutamate and GABA (4), may lead to positive or negative ions travelling through ion channels of the membrane to trigger or inhibit neurons.

To regulate these synaptic associated processes, there are neuromodulators of the synaptic activity, such as adenosine, which is also involved in key processes supporting cellular viability and adaptability, such as balancing the cellular energy charge or regulating metabolic pathways (5).

1.1.1. Adenosine and Adenosine Receptors

Adenosine is an endogenous purine nucleoside, present in all cells where it regulates important pathways in the primary metabolism. It is formed from catabolized adenosine 5’ – monophosphate (AMP), through cytosolic 5’ – nucleotidase, and may be phosphorylated back into AMP by adenosine kinase. Adenosine can also be metabolized extracellularly in the nervous system. Its presence in the extracellular media is originated both from its release from cells when intracellular concentration rises or from the extracellular dephosphorylation of adenine nucleotides (ATP) locally released, which appears to be one of the main sources of adenosine at the synaptic level (5–7).

Besides controlling neuronal excitability, synaptic plasticity, and neurodegeneration, adenosine also modulates neuronal activity, namely through its action in astrocytes and microglia (5).

Adenosine operates by interacting with G-protein coupled receptors (GPCR), adenosine receptors (ARs), expressed in several tissues, with particular high abundance in the brain. These membrane-associated receptors have seven putative transmembrane domains and exert their action through the activation of different signal transduction pathways (6,8). There are four different ARs: A_1, A_{2A}, A_{2B} and A_3. In normal conditions, extracellular adenosine binds to high affinity A_1 and A_{2A} receptors, unlike what happens to A_{2B} and A_3 low affinity receptors (9).

A_1 receptors (A_1Rs) are the most abundant and widespread adenosine receptors in the brain, being especially present in excitatory (glutamatergic) synapses (9). In physiological conditions, activation of A_1Rs modulates neuronal activity, inhibiting the excitatory neurotransmission and decreasing the neuronal excitability (10,11). Thus, A_1Rs are responsible for controlling basal synaptic transmission (12).

A_{2A} receptors (A_{2A}Rs) are present at higher levels in the basal ganglia and, like A_1Rs, in excitatory (glutamatergic) cortical synapses (13) throughout the brain. In basal conditions, A_{2A}Rs are engaged upon higher frequencies of stimulation, playing a crucial role in the control of synaptic efficiency in multiple brain regions. (14–16). Thus, A_{2A}Rs are selective controllers of adaptive alterations of synaptic plasticity (12).

The A_{2B} receptor has a low density in the brain, which indicates a possible role in pathological conditions (9). The A_3 receptor despite being highly abundant in peripheral tissue and shown to modulate synaptic activity in the hippocampus, is poorly understood and its effects on neuronal activity are still mostly unknown (7).

1.1.2. Neurodegeneration and A_{2A} Receptors

Different roles operated by adenosine in the brain demonstrate that it causes different and opposite effects, depending on which adenosine receptors (ARs) are activated. Generally, A_1Rs are described as neuroprotective whereas A_{2A}Rs are seen as potentially deleterious. This is associated to an increased density of A_{2A}Rs and decrease in the density of A_1Rs in several studies in different neurodegenerative diseases, such as Alzheimer's disease (14,17,18).

1.1.3. Alzheimer's Disease

Alzheimer's disease (AD) is primarily characterized as an evolving neurodegenerative disorder, with progressive loss of short-term reference memory, language disturbances (reading, speaking, writing) and impairment in executing daily routines (19). Characteristics of early stages of AD include memory and cognitive impairments coupled with emotional alterations. Also, it is observed a decreased metabolic activity in the cortex and hippocampus (20,21), which will be detailed in chapter 1.2, and a decreased size of these brain regions with disease progression (22,23).

Pathological hallmarks of AD are associated with the aggregation of amyloid-β protein (Aβ) in senile plaques, accumulation of hyperphosphorylated tau protein in neurofibrillary tangles and loss of neurons and synapses (24,25). But the morphological trait most commonly described at the onset of AD symptoms is the loss of synaptic density in the hippocampus and cortical regions (26,27).

Even though there is no cure nor treatment capable of slowing down or stopping AD progression, there are a few candidates therapeutic targets, such as A_{2A}Rs. In this way, several studies have converge concluding that the blockade of A_{2A}Rs offers a robust neuroprotection against brain damage, especially in cortical regions of the brain. Notably, A_{2A}Rs play a critical role in learning and memory mechanisms, which makes them relevant in AD. Several studies confirm this crucial role: I) the activation of A_{2A}Rs is necessary to trigger memory impairment in adult mice (12); II) a model of overexpression of A_{2A}Rs reported working memory deficits as well as alterations in synaptic plasticity (28); III) neuronal A_{2A}Rs are involved in early synaptic deficits detected in the AD mouse model APP/SP1 (29).

1.1.4. Neuroprotection and A_{2A} Receptors

Neuroprotection afforded by A_{2A}Rs blockade can be achieved by several mechanisms, namely by the use of an antagonist, like caffeine, or the genetic inactivation of A_{2A}Rs' gene *Adora 2A* (16).

Caffeine is the most widely consumed psychoactive substance, being known to improve attention and alertness, as well as to stabilize cognitive performance and mood. The beneficial effects of caffeine are associated with a moderated consumption, as higher doses induce a pattern of physiological and psychological reactions related to neurotic anxiety (30). Even though caffeine can have multiple targets, in non-toxic doses it is thought to mostly act as an

antagonist of adenosine receptors (31,32). Notably, the regular consumption of moderate doses of caffeine attenuates memory impairments upon aging and prevent features of characteristic of the onset AD (33,34), and that in hippocampus, A_{2A}Rs are responsible for regulating the impact of caffeine on the synaptic plasticity (32).

To study the neuroprotective effects of blocking A_{2A}Rs, a mouse model with a genetic inactivation in the gene *Adora2A*, which expresses these receptors, has been widely used: A_{2A}R knockout mice (A_{2A}R KO). A_{2A}R KO allowed to understand the important neurophysiological role of A_{2A}Rs in the brain, namely in the control of dopamine D_2R function in the striatum and the selective impact on synaptic plasticity, though not affecting the basal synaptic transmission in different brain area (35,36).

These neuroprotective mechanisms may also be associated with alterations of metabolic pathways in the brain, which will be reviewed in the following chapter.

1.2. Brain metabolism

Brain functioning involves a high metabolic activity required to provide energy for the process neurotransmission, namely energy to generate and propagate action potentials and for neurotransmitters' removal from the synaptic cleft. Neurons expends 70 – 80% of the total energy in the brain, and the additional amount is used by glial cells (37).

Glucose is believed to be the main source of energy to sustain neuronal activity, both in resting or activated states (38). Generally, the primary metabolism in the brain starts with the transport mainly of glucose into glia cells and neurons (39). Glucose enters the glycolytic pathway, where it is metabolized into two pyruvate molecules. Then, two main metabolic pathways are possible: aerobic oxidation, where pyruvate is actively transported into the mitochondria to be decarboxylated to acetyl coenzyme A (acetyl-CoA), which condensates with oxaloacetate, entering the TCA cycle, also known as Krebs cycle; or lactic acid fermentation, in which pyruvate is reduced to lactate (**Figure 1**). The aerobic oxidation permits a higher production of adenosine 5'-triphosphate (ATP), despite being slower compared to the glycolytic pathway, and also generates important metabolic intermediates required for biosynthetic processes, such as synthesis of neurotransmitters (37,40,41).

Neurons are considered mostly oxidative, whereas astrocytes are more glycolytic, meaning that most pyruvate originated from glycolysis enters the neuronal Krebs cycle (42). This can partially result from the expression, in neurons, of the low-pyruvate-affinity isoform of lactate dehydrogenase (LDH1), limiting the conversion of pyruvate into lactate and facilitating the oxidative pathway (43,44).

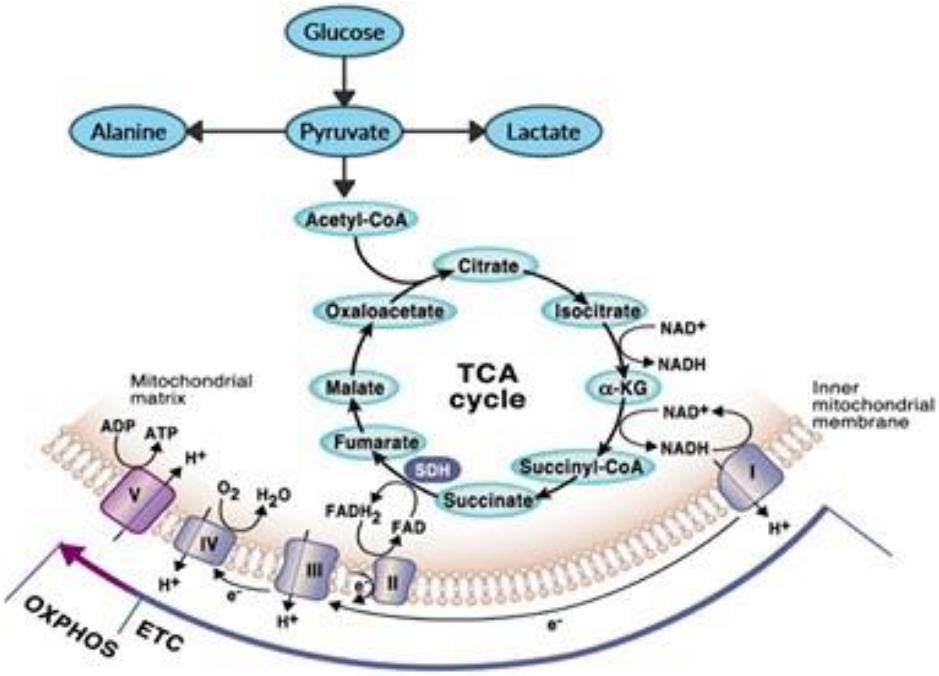

Figure 1: Two main metabolic pathways are represented: lactic acid fermentation and oxidative phosphorylation, adapted from (41).

Neurons and astrocytes have a distinct organization of primary metabolism, yet they are connected by the exchange of metabolites. One important connection between neurons and astrocytes is the glutamate-glutamine shuttle (45), necessary to fill glutamate losses caused by neurotransmission, and another important metabolic connection is the astrocyte-to-neuron lactate shuttle (46).

Glucose is not the only source of energy used by neurons, and there are several theories being tested as for other precursors/metabolites that can have a greater impact in metabolic activity such as lactate derived from the astrocyte-neuron lactate shuttle (46). In this shuttle, lactate produced by astrocytes is transferred to neurons where it is consumed as a substrate for oxidative metabolism (46,47). Taking a closer look at this process, it postulates that increased

neuronal activity leads to an increase on the extracellular concentration of glutamate taken up by astrocytes, via high affinity Na^+ dependent transporters, stimulating the metabolization of glucose to lactate (47,48). Also, increasing levels of glutamate and Na^+, activate glutamine synthetase and Na^+/K^+-ATPase, which leads to astrocytic ATP consumption (48). Then, there is the activation of anaerobic glycolysis, and the resulting lactate is transported from astrocytes into neurons (42,45), where it is converted back to pyruvate for ATP generation in mitochondria.

Such mechanism could regulate neurons' energy supply, as glutamate released from active neurons could stimulate generation of glycolytic ATP to support astrocytic uptake of glutamate and its conversion to glutamine, leading to lactate production (49). Some studies indicate that lactate can even replace glucose as a power source for neurons (50) , though the matter remains controversial.

In synapses, as in the whole brain, ATP is considered to be mostly generated by the complete oxidation of glucose, with estimations that mitochondria (oxidative phosphorylation) provide around 90 % of the ATP generated compared to only 10 % obtained from glycolysis (lactic acid fermentation) (49).

1.2.1. Metabolism, neurodegeneration, and Alzheimer's disease

There is increasing evidence suggesting that metabolic alterations strongly influence the onset and progression of neurodegenerative diseases (37). In fact, several disorders involve impaired energy metabolism and adverse changes in the cerebral vasculature, resulting in reduced energy availability to neurons, which can increase vulnerability of the brain to cognitive impairment and dementia.

In AD, one important process that is altered is glucose metabolism (37). Oxidative stress, due to an imbalance between reactive oxygen species (ROS) and reactive nitrogen species (RNS) formation and the availability of antioxidant defences, is known to promote AD progression as oxidative damage is increased in AD patients (51,52). One of the negative consequences of this increased oxidative damage is the glucose dysmetabolism, leading to an impaired ATP production by a decreasing mitochondrial flux and respiratory function (53). Evidences suggest that various enzymes are altered in the brain of AD patients, namely the mitochondrial aconitase, creatine kinase and ATP synthase (54,55). With diminished ATP production, the neuron's ability to maintain ionic gradients, for the production and propagation of action

potentials and neurotransmission is decreased, leading to synaptic dysfunction or even neuronal death.

In addition, some studies also indicate that in patients with mild cognitive impairments or early stages of AD, there are some changes in nutrient transporters and metabolic enzymes, such as a reduction in levels of GLUT1 and GLUT3 leading to diminished brain glucose uptake and subsequent cognitive decline (20,56), and loss of activities of several enzymes, like phosphofructokinase (PFK), pyruvate dehydrogenase complex, glucose-6-phosphate isomerase and lactate dehydrogenase (57,58).

The oxidative stress associated with AD originates from mitochondrial damage by the nitric oxide produced in response to amyloid β (Aβ) deposits (59), a hallmark of AD and, by an inhibition of mitochondrial movement by overexpression of Tau, a microtubule associated protein that is hyperphosphorylated in AD (60), constituting this the second hallmark of AD. Both mechanisms damage mitochondria within synapses, leading to disruption and decreased supply of energy to synapses and, as a result, synaptic dysfunction (49,61,62).

1.2.2. Metabolism and neuroprotection

Metabolism might also be involved in various neuroprotection mechanisms, such as the effects of caffeine or of $A_{2A}R$ blockade.

Converging evidence points out that caffeine, a non-selective antagonist of $A_{2A}R$, offers neuroprotection against cognitive and memory impairments related to neurodegenerative diseases, though the exact mechanisms and processes are not fully understood or known (16). Caffeine is involved in several mechanisms, ranging from ergogenic effects to metabolism and mitochondrial function.

As an ergogenic aid, caffeine has been shown to have beneficial effects in wakefulness, alertness and cognitive performance, especially during sleep deprivation (63), as well as in exercise performance, in which it increase the duration of the exercise and decreases the perception of fatigue (64,65). However, these beneficial effects are only observed with lower doses of caffeine, as higher doses can lead to the appearance of anxiety, psychomotor agitation, dysphoria, and insomnia (31,32). Moreover, chronic consumption of moderate doses of caffeine has a positive impact in AD and aging, by attenuating memory deterioration (31,34,66,67).

Furthermore, caffeine increases the rates of cerebral glucose utilization in both acute (10 mg/kg) and chronic consumption (2 weeks) (68,69), although it also decreases cerebral blood

flow (70). Duarte *et. al* (2009, 2012, 2019) (71–73), studied whether there were any induced hippocampal metabolic alterations associated with its apparent neuroprotective role in type 1 and type 2 diabetes. These studies revealed that caffeine prevented synaptic dysfunction and memory impairments in both types of diabetes (72), and at the same time showed that, hippocampal glucose content and transport were not altered in type 1 diabetes (71) and that metabolic changes induced by type 2 diabetes were not prevented by long-term consumption of caffeine, though both caffeine and type 2 diabetes had an impact on metabolism (73).

Notably, animals from both types of diabetes displayed increased hippocampal levels of taurine (71,73). Taurine is a non-essential amino-acid, present in large concentrations (mM) in the mammalian brain, that plays an important role as an osmolyte (74). In relation to diabetes, it has been described as a mitochondrial matrix buffer, preserving mitochondrial function (75). Moreover, caffeine controls taurine release from both neurons and glia through adenosine receptors (76), so a link between increased taurine levels and neuroprotection is pointed out (73).

Most neurodegenerative diseases, as mentioned before, are associated with oxidative stress and mitochondrial damage. The brain is more sensitive to the generated oxidative stress compared to other organs, due to the high amount of unsaturated fatty acids and lipids which can be considered as targets for lipid peroxidation (77). Caffeine is considered an anti-oxidant, inhibiting lipid peroxidation and reduce ROS production and, thus, having a positive effect as an antioxidant substance (78), therefore reducing oxidative stress and improving mitochondrial function (79). Moreover, long-term exposure to low doses of caffeine increases the cerebral glutathione (GSH) content, that is associated with neuroprotection (80,81).

$A_{2A}R$ blockade, as mentioned before, also affords neuroprotection (16). Extracellular adenosine levels increase drastically during brain insults (14). $A_{2A}Rs$ are upregulated in both neurons (72,82) and microglia (83), disrupting synaptic function and potentiating inflammatory cascades, and thus, blocking this receptor affords a robust neuroprotection (84). However, it remains to ascertain if a control of brain metabolism might underlie the neuroprotective action of caffeine and of $A_{2A}R$ blockade.

2. Aim

Several studies from patients and animal models indicate that most brain diseases begin with a dysfunction or loss of synapses, although the triggering mechanisms are still unknown. Since function and viability of any biological tissue is dependent on the ability of maintaining a primary metabolism that sustains its needs, metabolic impairments are, now posted to underlie synaptic dysfunction and loss.

The main purpose of this Master Thesis was to perform a metabolic analysis, selectively in cerebrocortical nerve terminals to understand the metabolic alterations underlying synaptic dysfunction in neurodegenerative disease, such as AD, as well as uncover if metabolic mechanisms accompanied neuroprotective processes (caffeine and $A_{2A}R$ blockade). To accomplish these goals, we took advantage of synaptosomes, a purified fraction of synapses and cortical slices. Two main tasks were established:

1 – Use of proton high-resolution NMR spectroscopy to compare the metabolic profile of cortical synaptosomes from a mouse model of AD and investigate the consumption of glucose *versus* lactate to identify particular metabolic features and preferences of nerve terminals.

2 - Use of proton high-resolution NMR spectroscopy to compare the metabolic profile of cortical synaptosomes *versus* cortical slices, subject to caffeine and genetic inactivation of $A_{2A}Rs$, to grasp alterations related to neuroprotection, with substrate competition (glucose *versus* lactate), and also perform an analysis of stable isotope incorporation in metabolic intermediates by ^{13}C NMR isotopomer analysis.

The selection of cortical tissue, although more heterogenous than other brain areas, is justified by its larger size to maximize the amount of tissue available for NMR spectroscopy analysis; the selection of mice, despite having a smaller brain size than rats, is justified by the number of transgenic animals modelling different neuropsychiatric disorders, like AD or other conditions such as selective genetic inactivation of $A_{2A}R$.

3. Materials and methods

3.1. Animal models

Mice were housed in groups of 2-4 per cage in a temperature-controlled room (22 ± 1°C), with free access to food and water, and with a 12 h light/12 h dark cycle (lights on at 7:00 am). Mice were handled to minimize not only animal suffering, but also the number of animals used in each study, being sacrificed by cervical dislocation and subsequent decapitation. All studies were conducted in accordance with the principles and procedures outlined as "3Rs" in the EU guidelines and animal experiments were approved by the Ethical Committee of the Centre for Neuroscience and Cell Biology of the University of Coimbra (CNC) – ORBEA n° 138-2016/15072016 – in accordance with the European Union (EU) directive 2010/63/EU.

3.1.1. Experiments on Animal models

Different animal models were utilized throughout the experiments: 3 and 9 months of age male $A_{2A}R$ knockout mice ($A_{2A}R$ KO) (85) and 6 and 9 months of age female double transgenic APP/PS1 mice (86), as well as sex and age-matching wild - type littermates (WT). In spite of sex dimorphism in some cardiovascular functions (87), brain maturation (88) and most recently, in the healing process (89) in $A_{2A}R$ KO mice, we chose to perform our experiments in males. As for APP/PS1, females were chosen due to the characteristic of our colony.

$A_{2A}R$ KO are characterized by a genetic inactivation of gene *Adora2A*, which is responsible for the expression of $A_{2A}Rs$, affording neuroprotection against brain damage, such as brain ischemia (90–92), without major impact on their development until adulthood (92), in spite of the role of $A_{2A}Rs$ in development of neuronal networks (93).

APP/PS1 mice (86), which mimics AD, were generated by co-injecting two vectors encoding mutant APP and PSEN1, being characterized by the appearance of Aβ deposits as well as memory and synaptic plasticity impairments (29,86). This animal model is associated with early - onset AD, as previously characterized by our research group (29).

3.1.2. Caffeine Treatment

Caffeine studies were conducted on 3 months old WT male mice, which were kept at room temperature (20°C - 25°C) in cages with *ad libitum* access to food and water. Mice were

divided in two groups - caffeine treated animals and control group – which were housed as pairs in each cage.

Caffeine was administered in the drinking water (0,3 g/L) to the caffeine treated group of animals, whereas the control group received regular drinking water. The treatment lasted for 14 days (chronic), starting at 10 weeks of age. During the treatment, weight and caffeine/water consumption were monitored each three days. To equal the amount of caffeine consumed in each cage and to avoid any impact of isolation, animals were sacrificed in pairs (two each day).

3.2. Biological Experiments

3.2.1. Nerve terminals (P2 synaptosomes)

In order to study the metabolic alterations occurring in synapses, namely in the cerebrocortical synapses, we took advantage of P2 synaptosomes, which correspond to a subcellular fraction of purified synapses that is both biochemical and metabolically competent and autonomous during up to 7 hours (94).

The protocol used was previously validated in our group (13,95,96) and based on the description by Dunkley P. *et al.*, 2008 (97). It begins with the homogenization of fresh brain cortex tissue in an isotonic sucrose-HEPES solution (see in chapter **3.5.**) at 4°C and pH 7.4, allowing the separation between nerve terminal and respective axon, followed by two differential centrifugations. The first low-speed centrifugation (3,000 x *g* for 10 min at 4°C) consists in the removal of nuclei and cell remains as a pellet, leaving the synaptosomes in the supernatant, whereas the second one (14,000 x *g* for 12 min at 4°C) pellets synaptosomes, myelin and mitochondria, leaving small synaptic vesicles and soluble remains in the supernatant. The pellet was re-suspended in 1 mL of a 45% (v/v) Percoll solution made up in Krebs HEPES solution (see in chapter **3.5.**). After centrifugation (16,000 x *g* for 2 min at 4°C), the top layer containing the synaptosomal fraction, was removed and re-suspended in Krebs HEPES solution (see in chapter **3.5.**) (97,98). Protein quantification was performed by a colorimetric method, BCA method, using BSA as a standard, and Pierce ™ BCA Protein Assay Kit (Pierce ™, Thermo Scientific ™). The synaptosomal suspensions were maintained on ice until use.

To study metabolic alterations in synaptosomes, several experiments were performed, namely for protocol optimization and competition between substrates. In all the experiments,

synaptosomes were incubated at 37°C for 7h (95% O_2 + 5% CO_2) in plates containing Locke's buffer (see in chapter **3.5.**) with labelled substrates: 5 mM [1,6-$^{13}C_2$] glucose (Cambridge Isotopes Laboratories, Inc) for the experiments of protocol optimization and 5 mM [U-^{13}C]glucose (Cambridge Isotopes Laboratories, Inc) and 2 mM [3-^{13}C]lactate (Cambridge Isotopes Laboratories, Inc) for substrates competition experiments. After the 7h incubation, a centrifugation (16,000 x *g* for 2 min at 4°C) was performed to separate medium and synaptosomes, so extracellular medium samples were prepared - 180 µL of media and 45 µL of sodium fumarate (10 mM), standard (80/20 relation) (see in chapter **3.5.**) – and stored at -20°C for future analysis by ^{1}H NMR spectroscopy. The extraction of water-soluble metabolites from synaptosomes (aqueous extracts) was performed using methanol/water (80/20 relation) (99,100), and the aqueous extract samples lyophilized and stored in a desiccator. Data from the aqueous extract samples are not shown as the intensity of peaks was too low and quantification was not possible.

3.2.2. Superfusion of Cortical Slices

To further investigate the metabolic alterations in the brain cortex as well as assess the existence of metabolic differences between synapses and the whole tissue, coronal cortical slices (400 µm) were prepared, which contain preserved neuronal networks (101,102), as well as glial cells. Coronal cortical slices were utilized to perform competition of substrates experiments.

After animal decapitation, the brain was rapidly removed onto a petri dish containing modified Krebs solution (see in chapter **3.5.**), and the isolated cortex transversely cut in 400 µm slices using a McIlwain tissue chopper. Cortical slices were left to recover in the modified Krebs solution (previously and continuously gassed with 95 % O_2 and 5 % CO_2 mixture) (see in chapter **3.5.**) during at least 45 min at room temperature to allow their complete metabolic recovery (103). Cortical slices, corresponding to half of the cortex tissue, were then transferred to a submerged chamber and superfused (3 mL/min), in a close-loop circuit, with the same gassed modified Krebs solution at 37 °C. After 60 min, so as to allow their stabilization, slices were superfused with a gassed modified Krebs solution, now containing ^{13}C labelled substrates, 5 mM [U-^{13}C]glucose (Cambridge Isotopes Laboratories, Inc) and 2 mM [3-^{13}C]lactate (Cambridge Isotopes Laboratories, Inc) for 7h.

In the end of the superfusion protocol, extracellular medium samples were prepared - 180 µL of media and 45 µL of sodium fumarate (10 mM), standard (80/20 relation) (see in chapter **3.5.**) – and stored at -20°C for future analysis by ^{1}H NMR spectroscopy. To obtain the

aqueous extracts of cortical slices, they were transferred to a previously frozen at porcelain grinder (-80°C) and 300 µL of 7% (v/v) perchloric acid (PCA) were added. The grinded tissue mixed with PCA was centrifuged (16,000 x *g* for 15 min at 4°C), and the supernatant, containing the water-soluble metabolites, was neutralized with a decreasing gradient of KOH concentrations (from 10 M to 0.01 M). Then, the aqueous extracts were centrifuged to remove the salt formed with the addition of KOH, lyophilised, and stored in a desiccator until used to perform ^{13}C NMR spectroscopy.

3.3. Nuclear Magnetic Resonance (NMR) Spectroscopy

Nuclear magnetic resonance (NMR) spectroscopy is an analytical technique widely used in metabolomics, as it is non-invasive and has high quantitative capabilities (104). To trace and quantify metabolic pathways and fluxes, NMR uses isotope-labelled substrates, tracers. These tracers are catabolized through different metabolic pathways and the degree of isotopic enrichment in the metabolites of interest allow us to assess the contribution of different metabolic pathways (104–106).

Lyophilised extracts were dissolved in 600 µL of $^{2}H_2O$ (Eurisotop, Cambridge Isotopes Laboratories, Inc) containing the standard, sodium fumarate (2 mM) (see in chapter **3.5.**). For both ^{1}H and ^{13}C NMR quantification of medium samples and aqueous extracts, respectively, sodium fumarate (2 mM) was used as an internal standard.

^{1}H NMR spectra obtained with a Varian VNMRS 600 MHz NMR (Agilent) spectrometer using a 3 mm inverse-detection probe, were acquired at 25 °C using a 30° pulse, 7183.9 Hz sweep width, 32768 number of points and 10 s of recycling time (3 s of acquisition time and 7 s pulse delay). These analyses were performed at Laboratório de Ressonância Magnética Nuclear (L-RMN) from Centro de Química de Coimbra at University of Coimbra, and I would like to thank them for kindly allowing me to use the facility.

^{1}H and ^{13}C NMR spectra for the substrate competition experiments were acquired with a Bruker 500 MHz Ultrashield Neo NMR spectrometer using a 5 mm TCI C/N Prodigy Cryo probe. These spectra were obtained at 25 °C using a 30° pulse, 5882 kHz spectral width, 65536 number of points and 10 s of recycling time (3 s of acquisition time and 7 s pulse delay) for ^{1}H NMR spectra, and using a 30120 Hz sweep width, 32768 number of points and 2 s of recycling time (1.5 s of acquisition time and 0.5 s pulse delay) for ^{13}C NMR spectra. These analyses were

performed at NMR facility CERMAX in ITQB-NOVA, and I would like to thank them for kindly allowing me to use the facility.

3.3.1. ^{1}H NMR quantification – Media samples

Medium samples from both set of experiments: protocol optimization and substrate competition experiments, as described below, were acquired by ^{1}H NMR spectroscopy for quantification. Two main metabolic pathways were evaluated: the glycolytic pathway/ lactic acid fermentation and the oxidative pathway (**Figure 2 – Panel A**). Even though the metabolic pathways evaluated on both experiments were the same, the metabolic parameters evaluated were different, as described below.

For the optimization protocol experiments, in which the tracer used was [1,6-$^{13}C_2$]glucose, four metabolic parameters were evaluated: glucose consumption, calculated by the disappearance of [1,6-$^{13}C_2$]glucose from the medium – measured around 5.35 ppm; lactate production, calculated by the appearance in the medium of [3-^{13}C]lactate satellites – measured around 1.4 ppm; and the percentages (%) of glycolysis and OXPHOS, calculated using the ratio between glucose consumption and lactate production.

For the substrate competition experiments, in which the two tracers used were [U-^{13}C]glucose and [3-^{13}C]lactate, three metabolic parameters were evaluated in the medium: acetate production, in which we quantified [1,2-$^{13}C_2$]acetate and [2-^{13}C]acetate, being originated from [U-^{13}C]glucose and [3-^{13}C]lactate, respectively – measured around 1.9-2.0 ppm; glucose and lactate consumption, calculated as mentioned above – measured around 5.4 ppm and 1.4-1.5 ppm, respectively; and the glycolytic index, calculated as the ratio between glucose consumption [U-^{13}C]glucose, and lactate production [U-^{13}C]lactate. In **Figure 2**, there is a schematic of the Krebs cycle summarising the expected isotopomer labelling patterns.

3.3.2. ^{13}C NMR analysis – Extracts samples

Glutamate C4 multiplet resonances, measured around 30-35 ppm in the ^{13}C-NMR spectra of tissue extracts, were used to estimate the contribution of [U-^{13}C]glucose for acetyl-CoA enrichment and Krebs cycle turnover. Acetyl-CoA enrichment was estimated by the ratio between the resonances originated from [U-^{13}C]glucose (C4D45 – from the first turn on Krebs cycle, and C4Q – corresponding to succeeding turns in Krebs cycle) and all the resonance in C4 glutamate. Krebs cycle turnover was estimated by the ratio of C4Q and C4D45. **Figure 2 – Panel B** represent the glutamate C4 resonance and its multiplets.

Line fitting was used in ^{1}H NMR quantification and ^{13}C NMR analysis to resolve the issues that arose from the overlapped peaks.

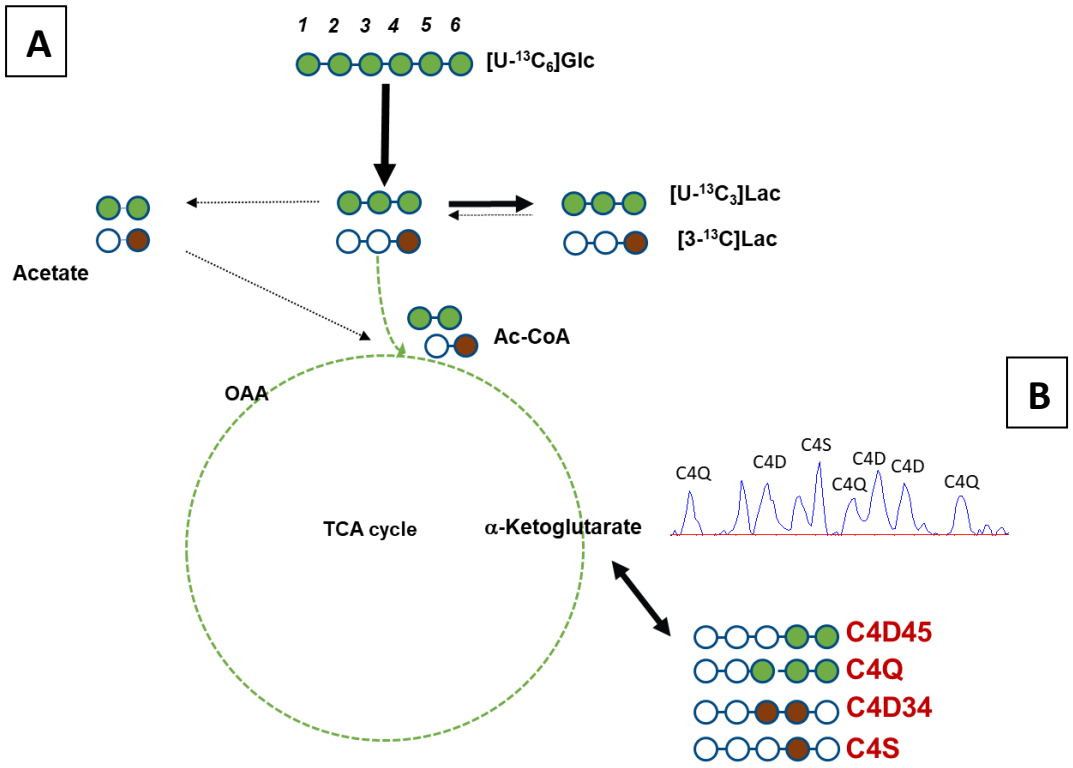

Figure 2: Two metabolic pathways are summarised in this picture: the glycolytic pathway (upper thick arrow), which involves the production of pyruvate from glucose then originating lactate and the oxidative pathway, in which pyruvate is converted to acetyl-CoA which enters the Krebs cycle (green lines) to be oxidized (**Panel A**). Glutamate C4 resonance in the ^{13}C-NMR spectra (**Panel B**). The circles painted represent labelled carbon (^{13}C) whereas the plain ones represent standard carbons (^{12}C) in the different molecules/ substrates. In green circles are represented substrates originated by [U-^{13}C]glucose and in brown the pathways from substrates originated by [3-^{13}C]lactate.

3.4. Statistics

The NMR spectra were analysed using two different software programs: NUTSpro™ (Acorn NMR) and TopSpin 4.0 (Bruker). For the ^{1}H NMR spectra, the areas of the signals from the metabolites were quantified by line fitting and the concentrations were determined by measuring the peak areas in the spectra, using sodium fumarate as the internal standard. In ^{13}C

NMR spectra, after line fitting, each multiplet area was reported as a fraction of the total area for that specific carbon resonance.

All the statistical analysis was performed using GraphPad Prism 8. In the data, each n accounts for 1 animal and no exclusion criteria were applied to outliers. Results are presented as mean ± SEM values of n experiments and statistical differences were considered at $p<0.05$. Generally, Student's *t* test was used to compare two data sets, and Two-way ANOVA followed by Sidak's post hoc test was used to compare two independent variables on a dependent variable.

3.5. Reagents and Solutions

- Sucrose HEPES solution – 0.32 M Sucrose; 1mM EDTA-Na; 10 mM HEPES; 1mg/mL bovine serum albumin (BSA)

- Krebs HEPES Ringer (KHR) solution – 140 mM NaCl; 1 mM EDTA-Na; 10 mM HEPES; 5 mM KCl; 5 mM glucose

- Percoll 45% - 45% (v/v) Percoll; 0.067 M NaCl; set volume with KHR

- Locke's Buffer – 154 mM NaCl; 5.6 mM KCl; 2.3 mM $CaCl_2$; 1 mM $MgCl_2$; 3.6 mM $NaHCO_3$; 5 mM HEPES + labelled substrates (5 mM [1,6-$^{13}C_2$] / 5 mM [U-^{13}C]glucose and 2 mM [3-^{13}C]lactate) + intermediaries pool solution

- Modified Krebs solution – 115 mM NaCl; 25 mM $NaHCO_3$; 3 mM KCl; 1.2 mM KH_2PO_4; 2 mM $CaCl_2$; 1.2 mM $MgSO_4$ + labelled substrates (5 Mm [U-^{13}C]glucose and 2 mM [3-^{13}C]lactate) + intermediaries pool solution

- Intermediaries pool solution – 0.2 mM malate; 0.002 mM aspartate; 0.02 mM α-ketoglutarate

- Sodium Fumarate – 143.98 mM NaH_2PO_4 + 56.02 mM Na_2HPO_4 in D_2O

All the reagents used in the experiments were purchased from Sigma - Aldrich, except for the labelled metabolites, [1,6-$^{13}C_2$]glucose, [U-^{13}C]glucose and [3-^{13}C]lactate from Cambridge Isotopes Laboratories, Inc.

4. Results

4.1. Protocol Optimization

In order to accomplish our goals and test the work hypothesis, some experiments were performed to build a protocol optimized to tackle our main goal. Firstly, we performed kinetic studies to select the incubation time needed for synaptosomes to reach metabolic steady state, then we evaluated the influence of two additional parameters through two separate sets of experiments: assess the effect of 4-aminopyridine (4-AP) to verify if stimulating the release of neurotransmitters had an impact on the primary metabolism of synaptosomes, and age-related studies, since aging is one of the major risk factors related to neurodegenerative diseases.

To determine the incubation time needed for synaptosomes to reach metabolic steady state, that is when the rate of consumption of a metabolite equals the rate of appearance of its products (107), while remaining viable and active, kinetic studies were conducted in 3 months old male $A_{2A}R$ KO (n=4) and WT littermates (n=4). Aliquots of incubation media, initially containing 5 mM of [1,6-$^{13}C_2$]glucose, were harvested at three different time points: 2h, 4h and 7h. The maximal time point evaluated was 7h, as 6-7h is the lifespan time of synaptosomes according to previous studies (94).

In **Figure 3** we can observe an increase in peak intensity for [3-^{13}C]lactate (one of the possible products of glycolysis, satellite at 1.42 ppm) both in WT and $A_{2A}R$ KO mice, with a concomitant increase in incubation time. Therefore, 7h was the time point selected as we have an increased production of [3-^{13}C]lactate without a significant increase of ^{12}C lactate leading us to assume that we are closer to metabolic steady state, and thus if we have more incorporation of tracer, leading to the appearance of [3-13C]lactate, the synaptosomes are still viable and active as their metabolic networks are functioning.

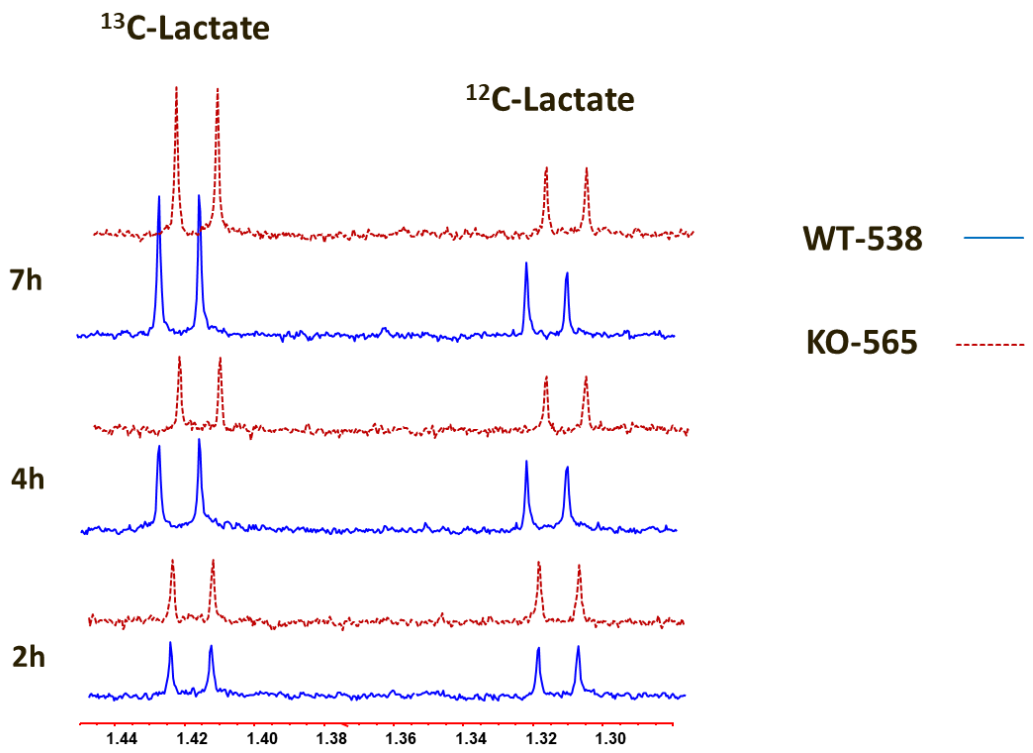

Figure 3: Typical ^{1}H-NMR spectra of incubation media samples from synaptosomes of male A_{2A}R KO (n=4) and male WT mice (n=4), in red and blue respectively, with 3 months, acquired in a Varian 600 MHz NMR spectrometer. There are three time points represented (2h, 4h and 7h) and the peaks represented are from [3–^{13}C]lactate and ^{12}C lactate with the purpose of indicating whether synaptosomes are metabolically competent and closer to metabolic steady state.

For the two other set of experiments, four metabolic parameters were evaluated, as mentioned in chapter **3.3.** from **Methods and Materials**: i) glucose consumption in µmol per mg of total protein from synaptosomes ii) lactate production in µmol per mg of total protein from synaptosomes and the percentages of iii) glycolysis and iv) OXPHOS, in which 100% corresponds to the total of [1,6-$^{13}C_2$]glucose being catabolized by either glycolysis or the oxidative pathway, respectively. It is important to notice that in these percentages, we are excluding other metabolic pathways for consumption of glucose besides glycolysis and oxidative phosphorylation pathway.

We assessed the effect of 50 µM of 4-aminopyridine (4-AP), concentration used on previous studies in synaptosomes (108) and hippocampal slices (109), to confirm whether stimulating the release of neurotransmitters had an impact on the primary metabolism of synaptosomes. For this experiment, cortical synaptosomes from male A_{2A}R KO mice (n=4) and

WT littermates (n=3) with 9 months were used, being incubated for 7h in Locke's buffer initially containing 5 mM of [1,6-$^{13}C_2$]glucose.

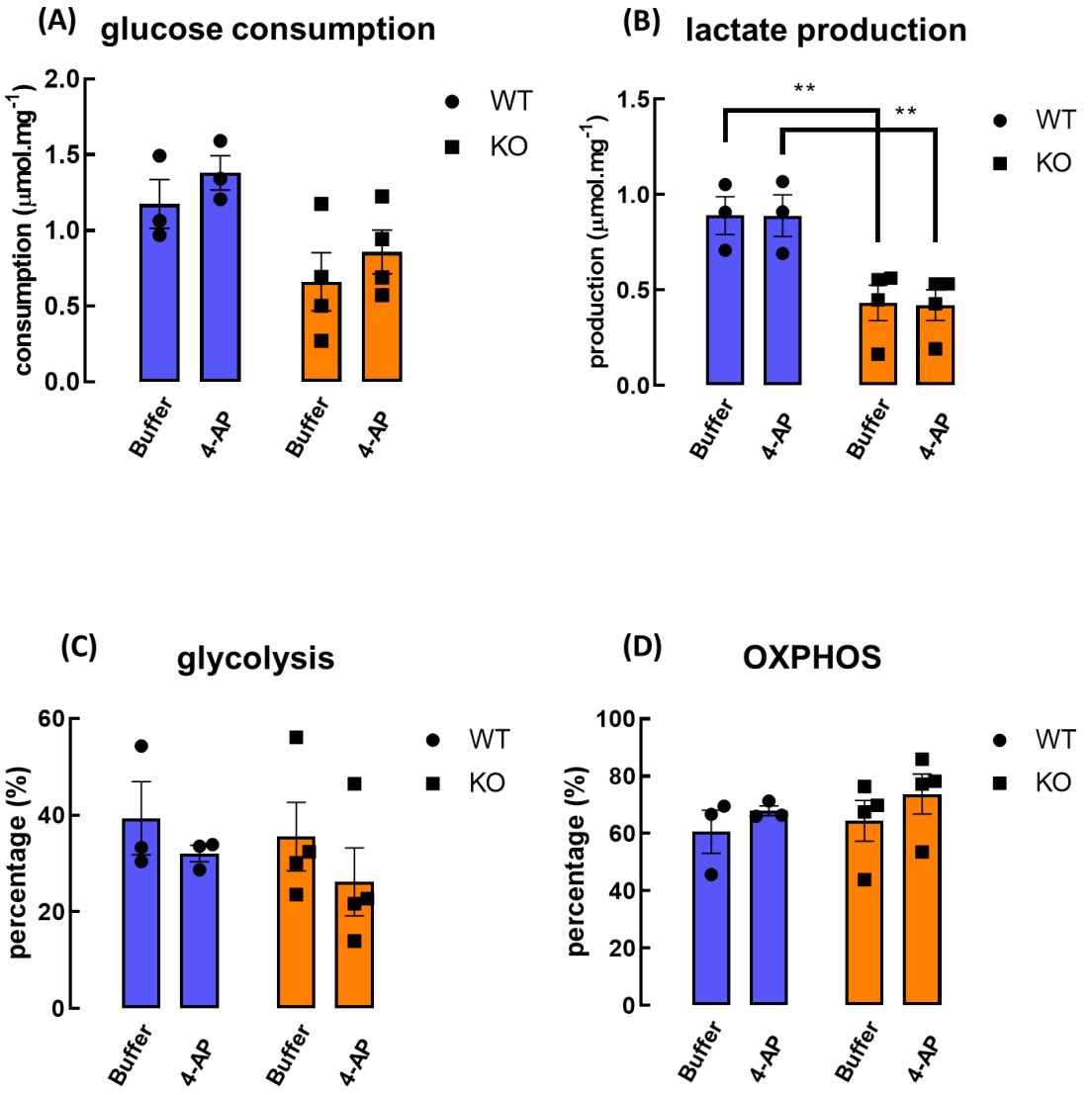

Figure 4: Parameters measured to evaluate metabolic alterations in cortical synaptosomes of male WT mice (n=3) and $A_{2A}R$ KO (n=4), in blue and orange respectively, in the absence (buffer) and presence of 50 µM 4-aminopyridine (4-AP)**.** Synaptosomes were incubated for 7h in Locke's buffer containing 5 mM [1,6-$^{13}C_2$]glucose. The parameters evaluated were: **(A)** quantity of [1,6-$^{13}C_2$]glucose consumed (µmol per mg of total protein content in synaptosomes); **(B)** quantity of [3-^{13}C]lactate produced from [1,6-$^{13}C_2$]glucose (µmol per mg of total protein content in synaptosomes); **(C)** % glycolysis – percentage of [1,6-$^{13}C_2$]glucose being metabolized in the glycolytic pathway; **(D)** % OXPHOS – percentage of [1,6-^{13}C]glucose being metabolized by oxidative phosphorylation pathway; In these percentages, 100% means that the total amount of labelled glucose is being consumed by that metabolic pathway. Data are presented as mean ± SEM and n=3-4 animals/group for all measured parameters. ** $p < 0.01$. Two-Way ANOVA followed by Sidak's *post hoc* test.

The results showed that glucose consumption varied ($p < 0.05$) according to genotype, namely a tendency of decrease between WT littermates and $A_{2A}R$ KO both in the absence and presence of 4-AP (**Figure 4(A)**). Lactate production was altered with genotype ($p < 0.001$); *post hoc* analysis confirmed a decrease in $A_{2A}R$ KO compared to WT mice both in the absence and presence of 4-AP ($p < 0.01$) (**Figure 4(B)**). Lastly, and despite the alterations observed in lactate production, there were no significant differences in the glycolytic or the oxidative metabolism (**Figure 4(C) (D)**).

Age-studies were conducted as aging has a high impact on neurodegenerative diseases (5). In this way, we compared results obtained from the previous experiences with synaptosomes from $A_{2A}R$ KO mice and WT littermates with 3 and 9 months. The results compared were cortical synaptosomes of WT littermates (n=4) and $A_{2A}R$ KO mice (n=4) with 3 months for the incubation time of 7h, and cortical synaptosomes of WT littermates (n=3) and $A_{2A}R$ KO mice (n=4) with 9 months in the absence of 4-AP.

The results showed that glucose consumption was altered ($p < 0.01$), being lower in the synaptosomes from $A_{2A}R$ KO with 9 months compared to 3 months ($p < 0.05$) (**Figure 5(A)**). As for lactate production, it varied according to genotype ($p < 0.05$), age ($p < 0.001$) and their interaction ($p < 0.01$); *post hoc* analysis confirmed that the production of lactate was significantly higher in synaptosomes from WT mice with 9 months compared to 3 months ($p < 0.001$), but also lower in synaptosomes from $A_{2A}R$ KO compared to WT mice with 9 months ($p < 0.01$) (**Figure 5(B)**). Finally, percentages of glycolysis and OXPHOS varied according to age ($p < 0.01$), with a significantly higher percentage of glycolysis in synaptosomes from both WT littermates and $A_{2A}R$ KO with 9 months compared to 3 months ($p < 0.05$) (**Figure 5(C)**), with a concomitant lower percentage of the OXPHOS pathway ($p < 0.05$) (**Figure 5(D)**).

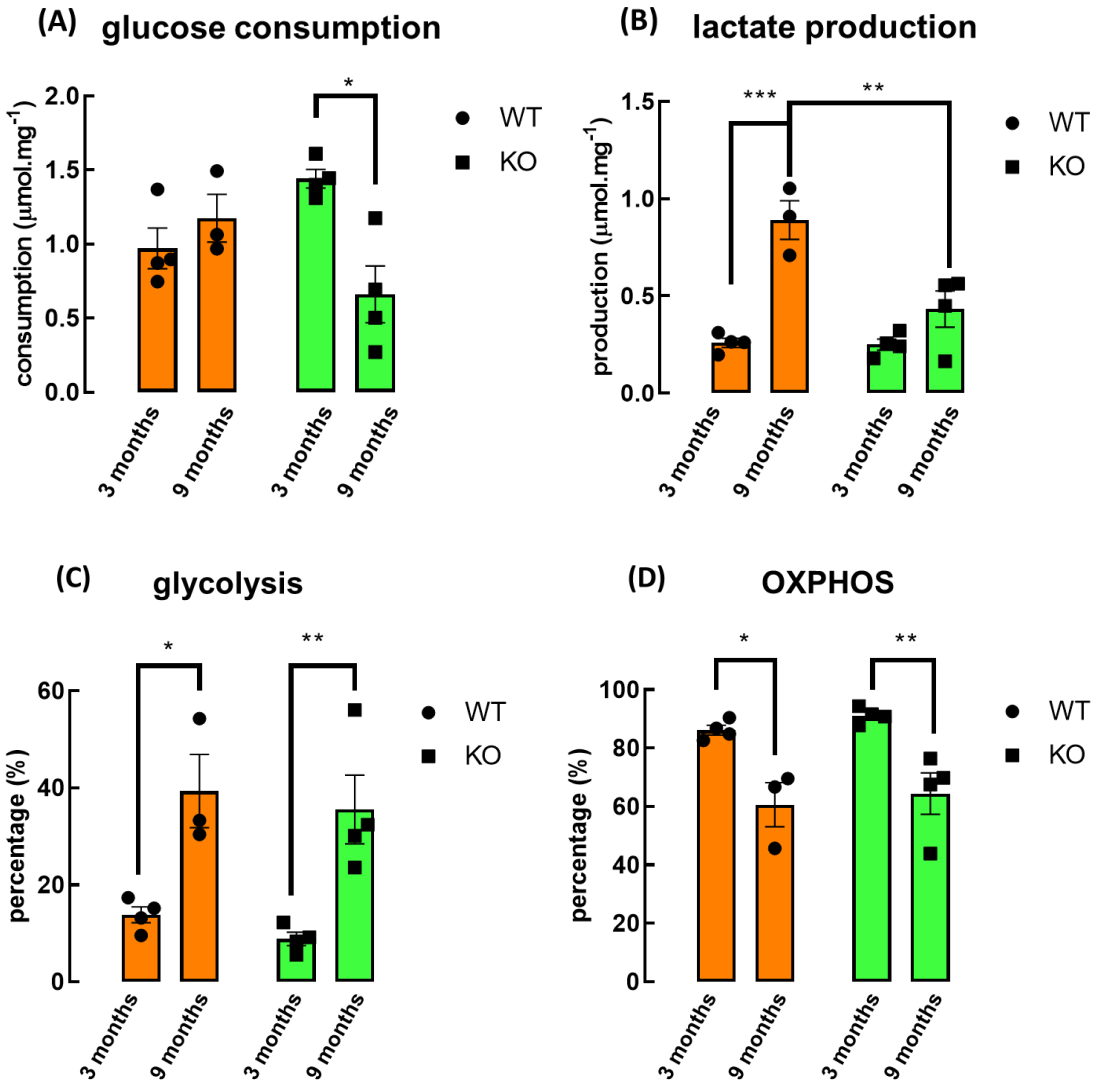

Figure 5: Parameters measured to evaluate metabolic alterations in cortical synaptosomes of male WT (n=3-4) mice and $A_{2A}R$ KO (n=4), in orange and green, respectively, with 3 and 9 months. Synaptosomes were incubated for 7h in Locke's buffer containing 5 mM [1,6-$^{13}C_2$]glucose. The parameters evaluated were: **(A)** quantity of [1,6-$^{13}C_2$]glucose consumed (µmol per mg of total protein content in synaptosomes); **(B)** quantity of [3-^{13}C]lactate produced from [1,6-$^{13}C_2$]glucose (µmol per mg of total protein content in synaptosomes); **(C)** % glycolysis – percentage of [1,6-$^{13}C_2$]glucose being metabolized in the glycolytic pathway; **(D)** % OXPHOS – percentage of [1,6-$^{13}C_2$]glucose being metabolized by oxidative phosphorylation pathway; In these percentages, 100% means that the total amount of labelled glucose is being consumed by that metabolic pathway. Data are presented as mean ± SEM and n=3-4 animals/group for all measured parameters. * $p < 0.05$; ** $p < 0.01$; *** $p < 0.001$. Two-Way ANOVA followed by Sidak's *post hoc* test.

4.2. Synapses in Alzheimer's Disease

Having the protocol established, two different sets of experiments were performed in cortical synaptosomes from APP/PS1, the mouse model that mimics AD phenotype (91), to understand whether there were any specific metabolic alterations in synapses in the early stages of AD.

In this way, we evaluated the metabolic parameters of cortical synaptosomes from 6 months APP/PS1 female mice (n=4) and WT littermates (n=3), with Locke's buffer containing 5 mM of [1,6-$^{13}C_2$]glucose, and then we performed the substrate competition experiment in cortical synaptosomes from 9 months APP/PS1 female mice (n=7) and WT littermates (n=5), with Locke's buffer containing 5 mM of [U-^{13}C]glucose and 2 mM of [3-^{13}C]lactate. In both experiments, cortical synaptosomes were incubated for 7h, the time point chosen in the protocol optimization experiments.

For the first experiment, the parameters evaluated were the same as for the previous experiences: i) glucose consumption in µmol per mg of total protein from synaptosomes ii) lactate production in µmol per mg of total protein from synaptosomes and the percentages of iii) glycolysis and iv) OXPHOS, in which 100% corresponds to the total of [1,6-$^{13}C_2$]glucose being catabolized by either glycolysis or the oxidative pathway, respectively. It is important to notice that in these percentages, we are excluding other metabolic pathways for glucose besides glycolysis and oxidative phosphorylation pathway.

The results showed that none of the metabolic parameters evaluated was altered **(Figure 6)**.

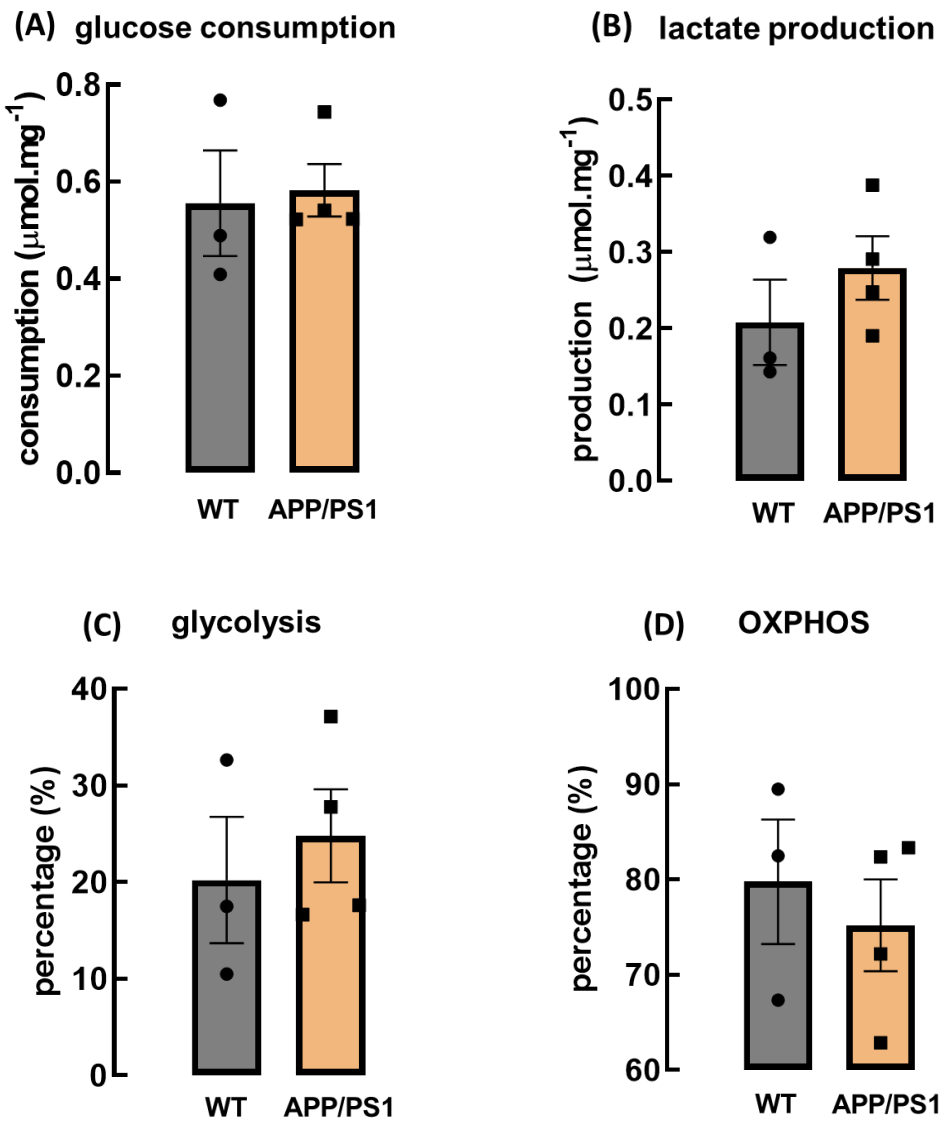

Figure 6: Parameters measured to evaluate metabolic alterations in cortical synaptosomes of 6 months female WT (n=3) and APP/PS1 mice (n=4), grey and light pink respectively, being incubated for 7h in Locke's buffer containing 5 mM [1,6-$^{13}C_2$]glucose. The parameters evaluated were: **(A)** quantity of [1,6-$^{13}C_2$]glucose consumed (µmol per mg of total protein content in synaptosomes); **(B)** quantity of [3-^{13}C]lactate produced from [1,6-$^{13}C_2$]glucose (µmol per mg of total protein content in synaptosomes); **(C)** % glycolysis – percentage of [1,6-$^{13}C_2$]glucose being metabolized in the glycolytic pathway; **(D)** % OXPHOS – percentage of [1,6-$^{13}C_2$]glucose being metabolized by oxidative phosphorylation pathway; In these percentages, 100% means that the total amount of labelled glucose is being consumed by that metabolic pathway. Data are presented as mean ± SEM and n=3-4 animals/group for all measured parameters. Student's unpaired *t* test.

Afterwards, we performed substrate competition studies using cortical synaptosomes from 9 months APP/PS1 and age-matched WT littermates. For this experiment, synaptosomes were incubated for 7h, in Locke's buffer containing 5 mM [U-^{13}C]glucose and 2 mM [3-^{13}C]lactate. Different metabolic parameters were evaluated: acetate production, in which we consider that if acetate is being produced, then acetyl-CoA is also being produced and assume that the highest producer of acetate is also the highest producer of acetyl-CoA that enters the Krebs cycle (µmol per mg of total protein from synaptosomes); glucose and lactate consumption (µmol per mg of total protein from synaptosomes); and glycolytic index.

The results revealed that acetate production was altered in label ($p < 0.001$) and in the interaction between label and genotype ($p < 0.05$); *post hoc* analysis confirmed that the production of [2-^{13}C]acetate was higher in synaptosomes from APP/PS1 compared to WT mice ($p < 0.05$), and that the production of [2-^{13}C]acetate was also increased in both WT littermates ($p < 0.05$) and APP/PS1 ($p < 0.001$) compared to the production of [1,2-$^{13}C_2$]acetate (**Figure 7(A)**). As for glycolytic index and [U-^{13}C]glucose and [3-^{13}C]lactate consumption, no variation was observed between WT and APP/PS1 (**Figure 7(B) (C)**).

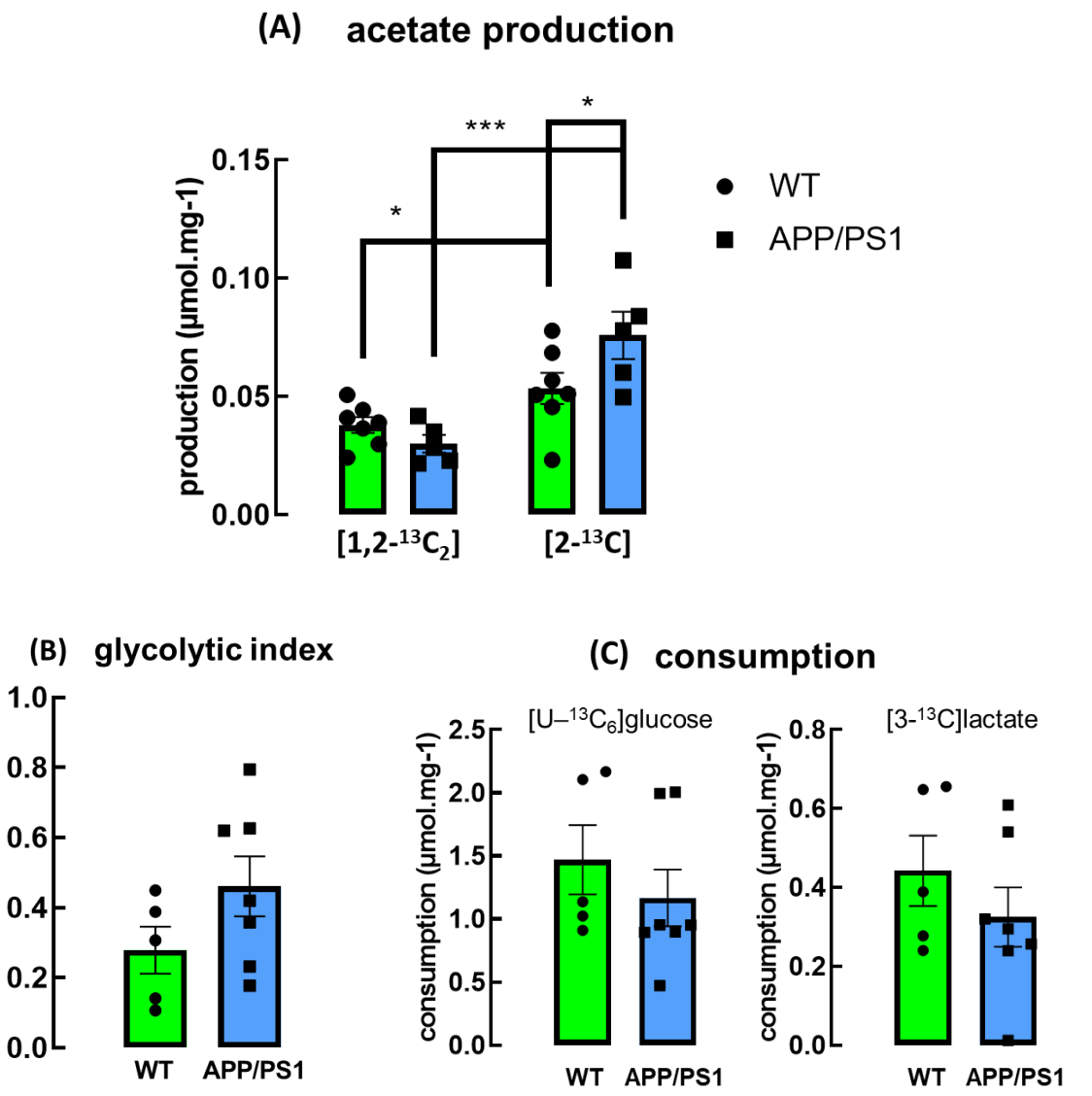

Figure 7: Parameters measured to evaluate metabolic alterations in cortical synaptosomes of 9 months female WT (n=5) and APP/PS1 (n=7) mice, green and blue respectively, being incubated for 7h in Locke's buffer containing 5 mM [U-^{13}C]glucose and 2 mM [3-^{13}C]lactate. The parameters evaluated were: **(A)** quantity of [1,2-$^{13}C_2$] and [2-^{13}C]acetate produced from [U-^{13}C]glucose and [2-^{13}C]lactate, respectively (µmol per mg of total protein content in synaptosomes) **(B)** glycolytic index, ratio corresponding to the [U-^{13}C]glucose being metabolized in the glycolytic pathway **(C)** quantity of [U-^{13}C]glucose and [3-^{13}C]lactate consumed (µmol per mg of total protein content in synaptosomes). Data are presented as mean ± SEM and n=5-7 animals/group for all measured parameters. * $p < 0.05$; *** $p < 0.001$. Two-Way ANOVA followed by Sidak's *post hoc* test; Student's unpaired *t* test.

4.3. Neuroprotection: Caffeine and $A_{2A}R$ KO

The next set of experiments were performed in both cortical synaptosomes and cortical slices, which were superfused, obtaining medium and tissue extract samples to be analysed through ^{1}H and ^{13}C NMR spectroscopy, respectively.

We performed a substrate competition experiment for both studies, so the parameters evaluated were the same for the cortical synaptosomes and slices: acetate production, in which we consider that if acetate is being produced, then acetyl-CoA is also being produced and assume that the highest producer of acetate is also the highest producer of acetyl-CoA that enters the Krebs cycle (µmol per mg of total protein from synaptosomes); glucose and lactate consumption (µmol per mg of total protein from synaptosomes); and glycolytic index, which indicates the amount [U-^{13}C]glucose being metabolized in the glycolytic pathway.

4.3.1. Neuroprotection: Caffeine

Caffeine offers neuroprotection against brain damage through binding with $A_{2A}Rs$ (31), so we conducted a study to understand whether there were alterations in the primary metabolism in synapses and brain when chronic caffeine treatment was applied.

These studies were performed in synaptosomes and slices from 3 months of age male WT littermates, divided into two groups: the first one subjected to 14 days of 0.3 g/L caffeine consumption and the other one the control group.

For cortical synaptosomes we had n=5 for the caffeine treated group as well as for the control group, having performed a substrate competition experiment, so Locke's buffer contained 5 mM [U-^{13}C]glucose and 2 mM [3-^{13}C]lactate.

The results showed that acetate production varied in label ($p < 0.001$); *post hoc* analysis established a greater [2-^{13}C]acetate production compared to the production of [1,2-^{13}C]acetate both in control ($p < 0.05$) and caffeine treated group ($p < 0.01$) (**Figure 8(A)**). For the other parameters evaluated, glycolytic index (**Figure 8(B)**) and [U-^{13}C]glucose and [3-^{13}C]lactate consumption (**Figure 8(C)**) no changes were observed due to label nor treatment ($p > 0.05$).

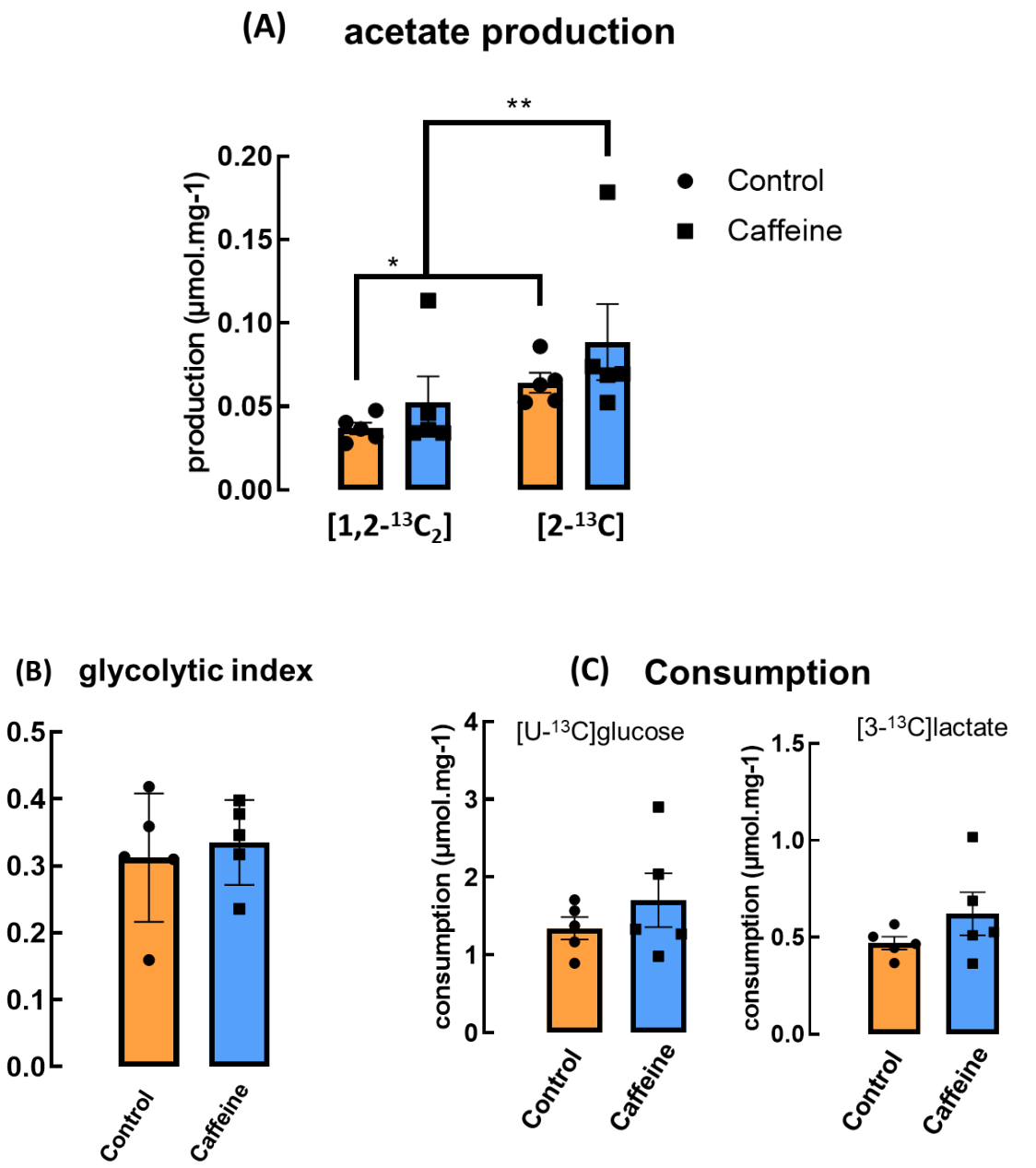

Figure 8: Metabolic parameters evaluated in cortical synaptosomes from male 3 months old WT littermates subject to chronic treatment for 14 days with 0.3 g/L caffeine (n=5) and age-matched controls (n=5), blue and orange respectively, being incubated for 7h in Locke's buffer containing 5 mM [U-^{13}C]glucose and 2 mM [3-^{13}C]lactate. The parameters evaluated were: **(A)** total amount of [1,2-$^{13}C_2$] and [2-^{13}C]acetate produced from [U-^{13}C]glucose and [2-^{13}C]lactate, respectively (µmol per mg of total protein content in synaptosomes); **(B)** glycolytic index, ratio corresponding to the amount of [U-^{13}C]glucose metabolized in the glycolytic pathway ; **(C)** quantity of [U-^{13}C]glucose and [3-^{13}C]lactate consumed (µmol per mg of total protein content in synaptosomes). Data are presented as mean ± SEM and n=5 animals/group for all measured parameters. * $p < 0.05$; ** $p < 0.01$. Two-Way ANOVA followed by Sidak's *post hoc* test; Student's unpaired *t* test.

For cortical slices we had n=3-4 for the caffeine treated group and n=5 for control group, having performed a substrate competition experiment, so modified Krebs solution contained 5 mM [U-^{13}C]glucose and 2 mM [3-^{13}C]lactate.

From the metabolic parameters that were supposed to be evaluated, acetate production in this experiment, was not possible to quantify as the signal-to-noise ratio corresponding to [1,2-^{13}C] and [2-^{13}C]acetate , in the ^{1}H NMR spectra, was very low. As for the other metabolic parameters, glycolytic index and [1,2-^{13}C]glucose and [2-^{13}C]lactate consumptions, similarly to the experiments on synaptosomes, no alterations were observed (**Figure 9**).

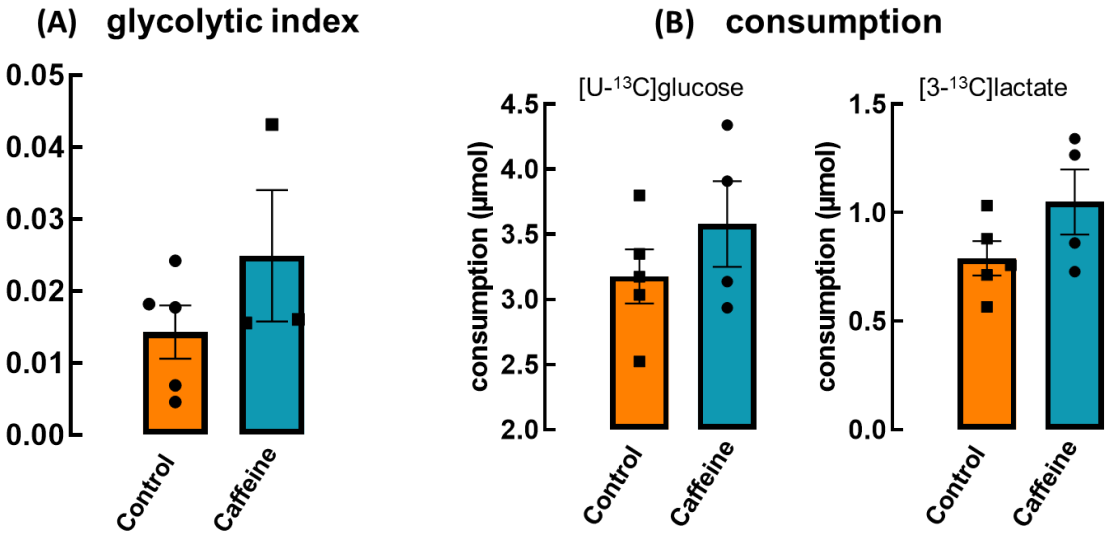

Figure 9: Metabolic parameters assessed in superfused slices from male WT littermates with 3 months, subjected to chronic treatment for 14 days with 0.3 g/L caffeine (n=3-4) and age-matched controls (n=5), blue and orange respectively, being superfused for 7h in a gassed modified Krebs solution containing 5 mM [U-^{13}C]glucose and 2 mM [3-^{13}C]lactate. The parameters evaluated were: **(A)** glycolytic index - ratio corresponding to the amount of [U-^{13}C]glucose metabolized in the glycolytic pathway; **(B)** quantity of [U-^{13}C]glucose and [3-^{13}C]lactate consumed (µmol). Data are presented as mean ± SEM and n = 3-5 animals/group for all measured parameters. Student's unpaired *t* test.

.

Despite the nonexistence of metabolic alterations in slices extracellular medium samples, ^{13}C NMR analysis was performed in tissue extracts from cortical slices. These experiences were carried out to have a more detailed information on which substrate, [U-^{13}C]glucose or [3-^{13}C]lactate, have the greater contribution to the oxidative pathway.

As mentioned in chapter **3.3.2**., two parameters were evaluated by looking at the carbon 4 of glutamate: [U-^{13}C] glucose contribution to the enrichment of [1,2-$^{13}C_2$]acetyl-CoA and the Krebs cycle turnover (**Figure 10**).

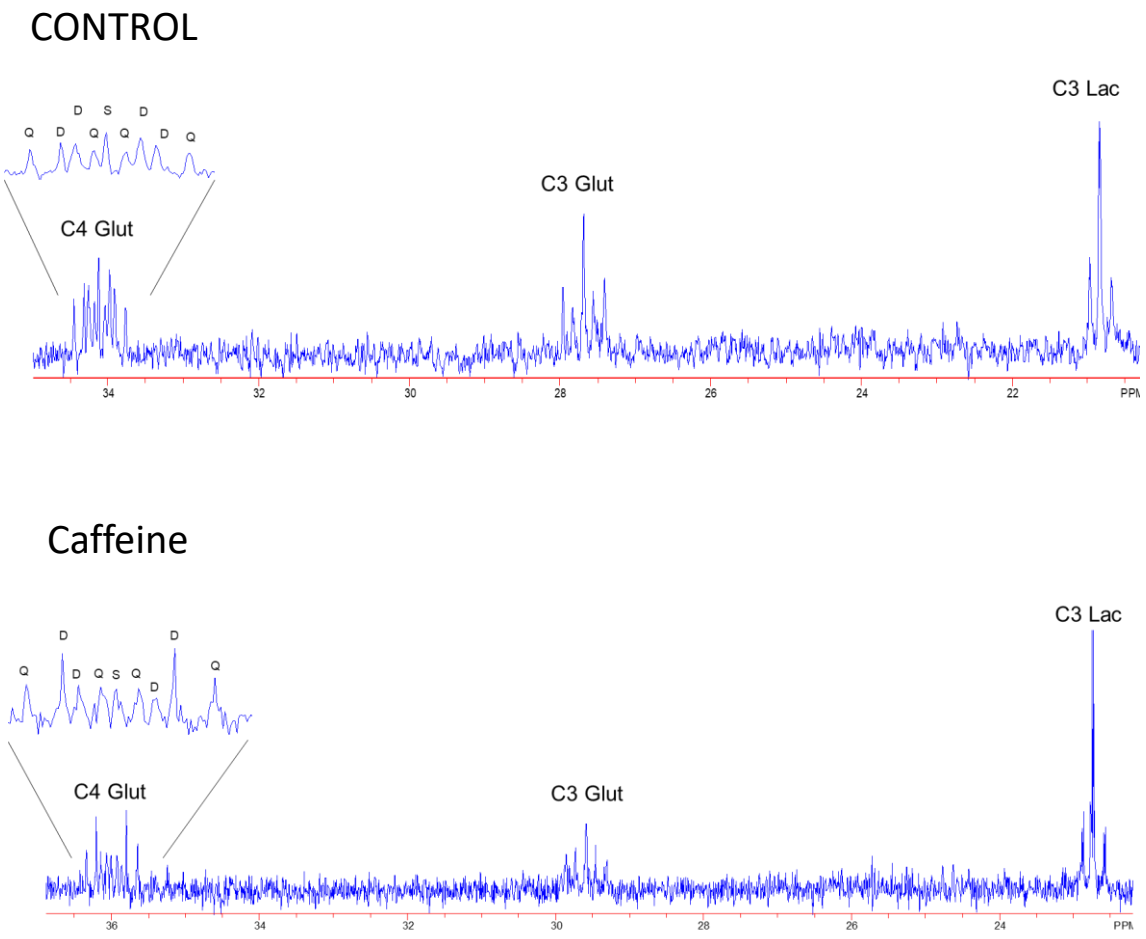

Figure 10: ^{13}C NMR spectra from two different samples: control and treatment with caffeine. There are three carbons from different metabolites identified: C4 and C3 from glutamate (left and middle) and C3 from lactate (right). The multiplets analysed were from the C4 of glutamate, which indicate the turnover of the Krebs cycle and thus of the prevalence of the oxidative pathway.

In the metabolic parameters evaluated, there were no significant changes (n=2 for both groups), although the results show a tendency for a higher contribution of [U-^{13}C]glucose to Ac-CoA in the group of animals treated with caffeine compared to controls, which is not reflected on the Krebs cycle turnover, where no alterations are observed (**Figure 11**). Nevertheless, the n number was too low to obtain a firm result.

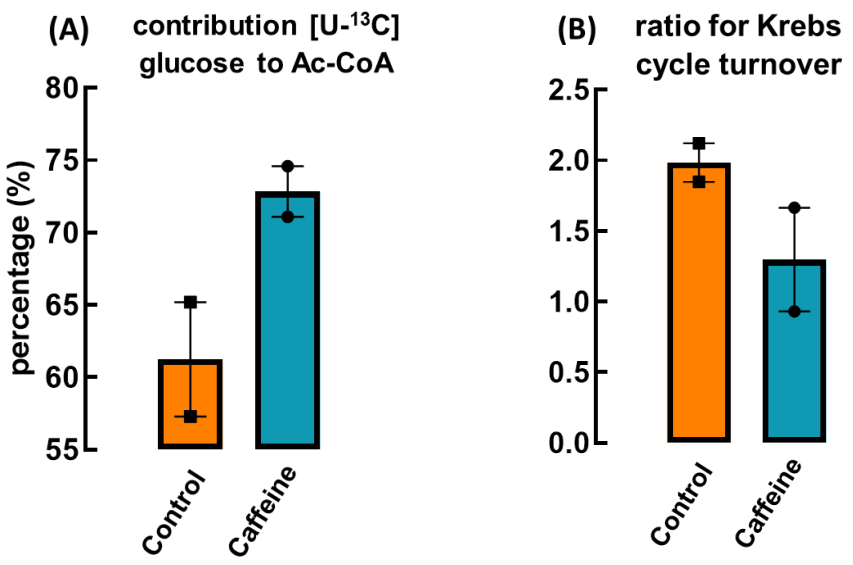

Figure 11: Metabolic parameters evaluated through ^{13}C NMR spectra of cortical tissue extracts from male WT littermates with 3 months, subjected to chronic treatment for 14 days with 0.3 g/L caffeine and age-matched controls, blue and orange respectively. The parameters evaluated were: **(A)** contribution of [U-^{13}C]glucose to the enrichment of acetyl-CoA; **(B)** Ratio of Krebs cycle turnover. Data are presented as mean ± SEM and n=2 animals/group for all measured parameters. Student's unpaired *t* test.

4.3.2. Neuroprotection: $A_{2A}R$ knockout animals

Similarly to caffeine, blockage of $A_{2A}Rs$ also offers neuroprotection against brain damage, especially associated with an increase in cognitive and memory performance (9,14,16). In this way, we assessed the same metabolic parameters evaluated in the caffeine experiments, but using 3 months old male $A_{2A}R$ KO and age-matched WT littermates. The concentrations used for the substrate competition being the same: 5 mM [U-^{13}C]glucose and 2 mM [3-^{13}C]lactate.

In cortical synaptosomes, acetate production was varied in label ($p < 0.01$); *post hoc* analysis indicated that the production of [2-^{13}C]acetate was diminished compared to [1,2-$^{13}C_2$]acetate production, both in WT littermates and $A_{2A}R$ KO ($p < 0.05$) (**Figure 12(A)**). For the other metabolic parameters evaluated, glycolytic index and [U-^{13}C]glucose and [3-^{13}C]lactate consumption, no alterations were observed (**Figure 12(B) and (C)**).

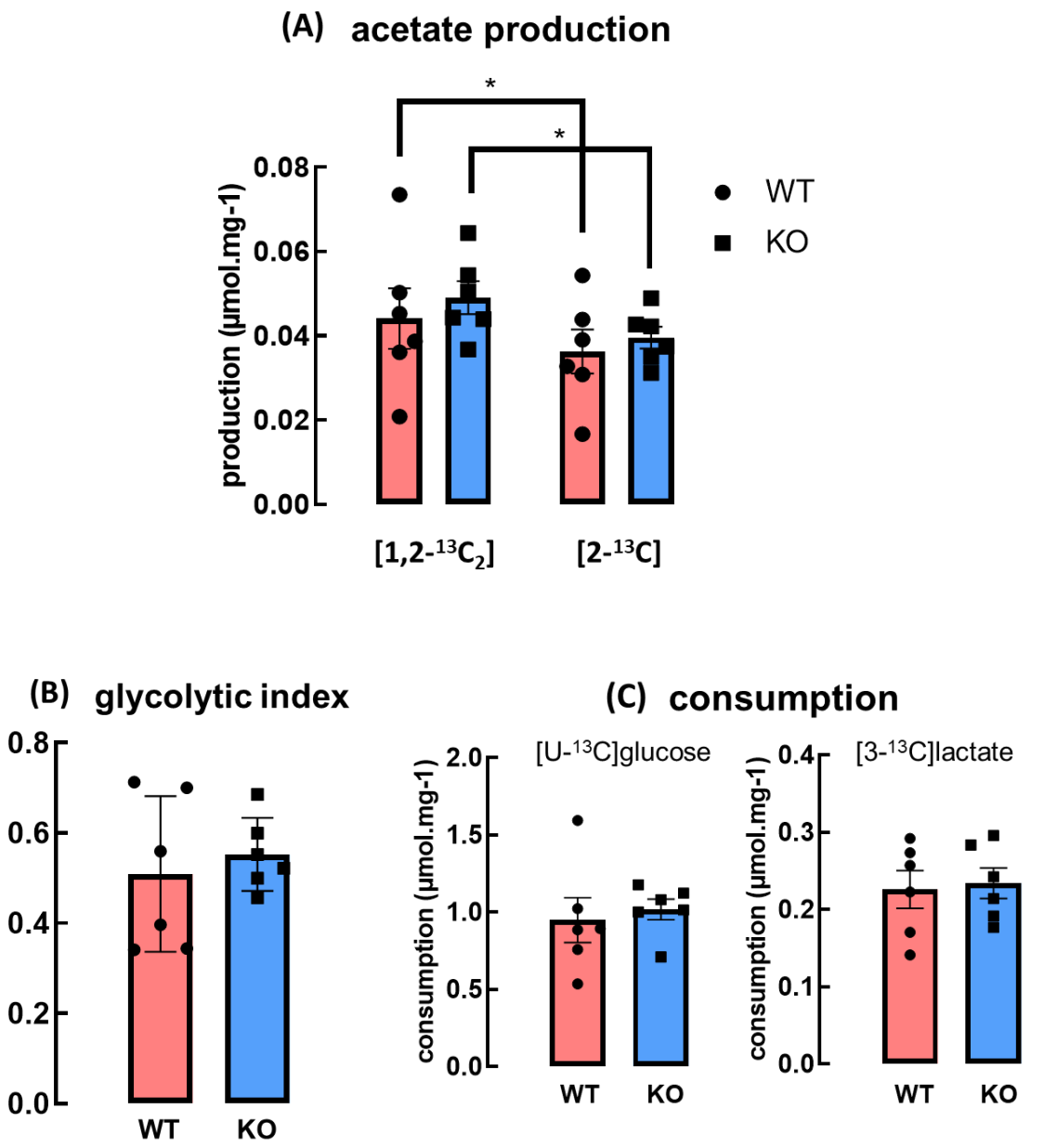

Figure 12: Metabolic parameters evaluated in cortical synaptosomes from male 3 months old WT littermates and $A_{2A}R$ KO, pink and blue respectively, being incubated for 7h in Locke's buffer containing 5 mM [U-^{13}C]glucose and 2 mM [3-^{13}C]lactate. The parameters evaluated were: **(A)** total amount of [1,2-$^{13}C_2$] and [2-^{13}C]acetate produced from [U-^{13}C]glucose and [2-^{13}C]lactate, respectively (µmol per mg of total protein content in synaptosomes); **(B)** glycolytic index, ratio corresponding to the amount of [U-^{13}C]glucose metabolized in the glycolytic pathway; **(C)** quantity of [U-^{13}C]glucose and [3-^{13}C]lactate consumed (µmol per mg of total protein content in synaptosomes). Data are presented as mean ± SEM and n=6 animals/group for all measured parameters * $p < 0.05$. Two-Way ANOVA followed by Sidak's *post hoc* test; Student's unpaired *t* test.

As for the cortical slices, and despite the metabolic differences observed in the production of acetate in cortical synaptosomes, no significant changes were observed in each of the three metabolic parameters evaluated. (**Figure 13**).

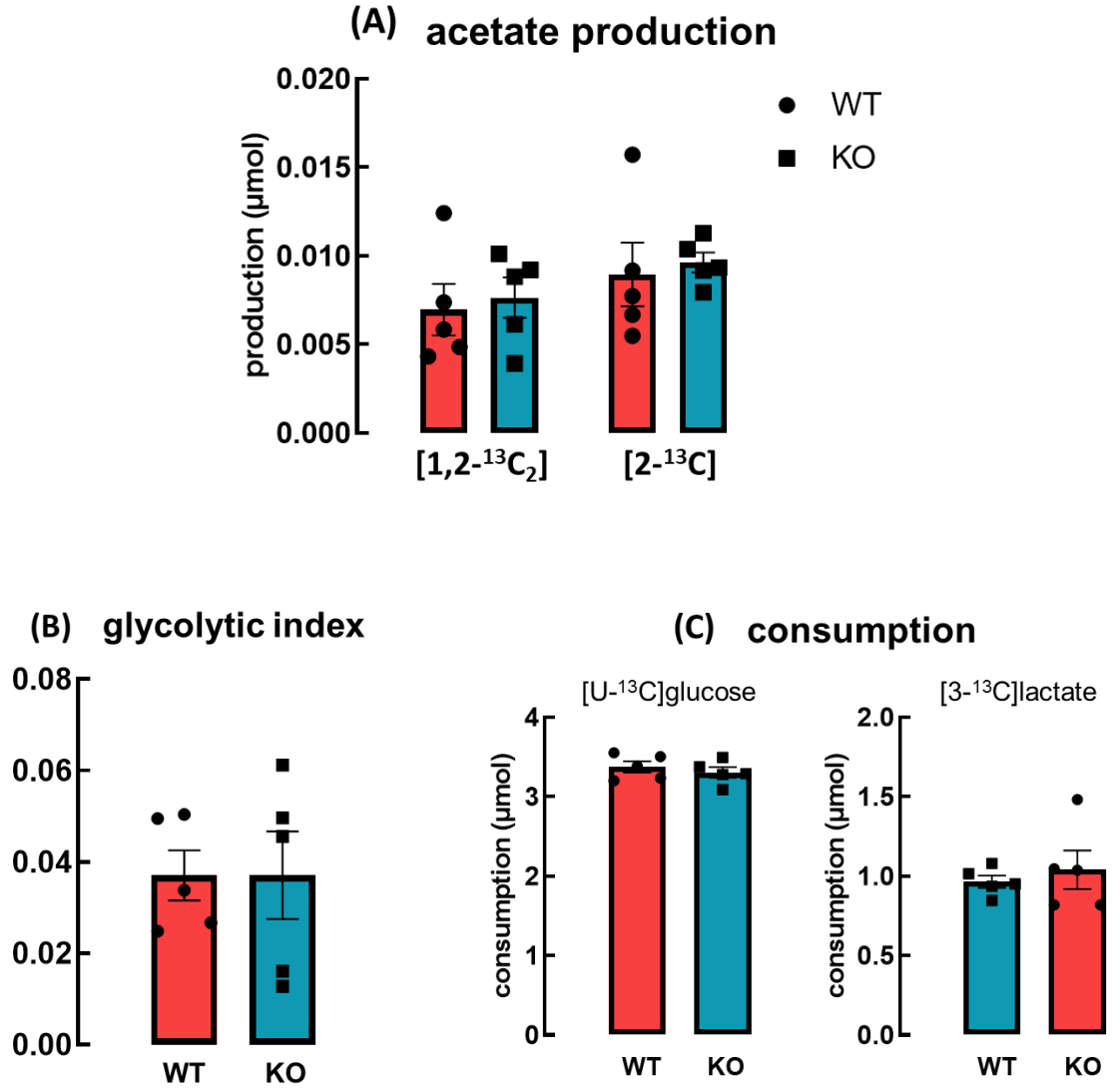

Figure 13 Metabolic parameters evaluated in cortical slices from male 3 months old WT littermates and $A_{2A}R$ KO, pink and blue respectively, being incubated for 7h in Locke's buffer containing 5 mM [U-^{13}C]glucose and 2 mM [3-^{13}C]lactate. The parameters evaluated were: **(A)** total amount of [1,2-$^{13}C_2$] and [2-^{13}C]acetate produced from [U-^{13}C]glucose and [2-^{13}C]lactate, respectively (µmol); **(B)** glycolytic index - ratio corresponding to the amount of [U-^{13}C]glucose metabolized in the glycolytic pathway; **(C)** quantity of [U-^{13}C]glucose and [3-^{13}C]lactate consumed (µmol). Data are presented as mean ± SEM and n=5 animals/group for all measured parameters. Two-Way ANOVA. Student's unpaired *t* test.

Next, ^{13}C NMR experiments were performed in cortical tissue extracts, and the parameters evaluated were the same as for the caffeine experiments. (**Figure 14**).

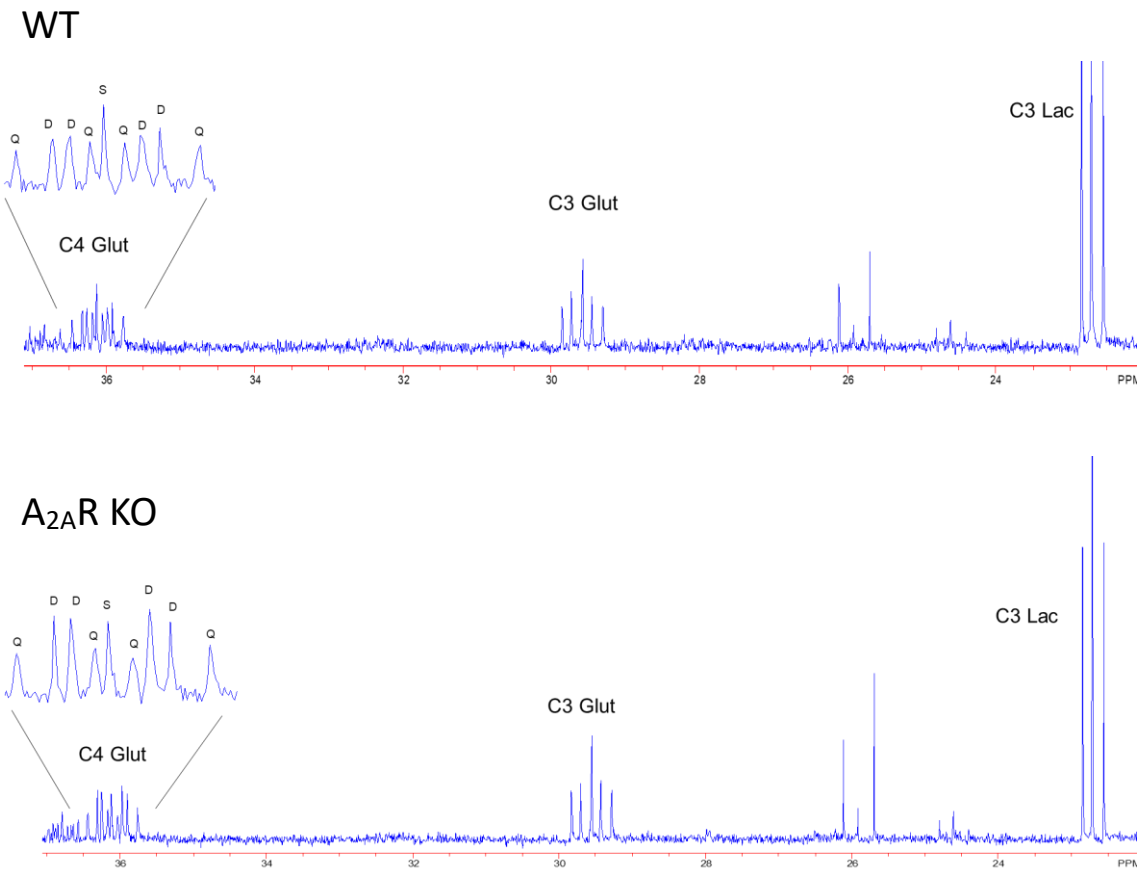

Figure 14: ^{13}C NMR spectra from two different samples WT and $A_{2A}R$ KO. There are three carbons from different metabolites identified: C4 and C3 from glutamate (left and middle) and C3 from lactate (right). The multiplets analysed were from the C4 of glutamate, which indicate the turnover of the Krebs cycle and thus of the prevalence of the oxidative pathway.

The same way as for caffeine experiments, due to the low number of samples analysed (n=2), none of the parameters assessed revealed alterations, although it appears to be a tendency of decrease in the Krebs cycle turnover in $A_{2A}R$ KO compared to WT littermates (**Figure 15**).

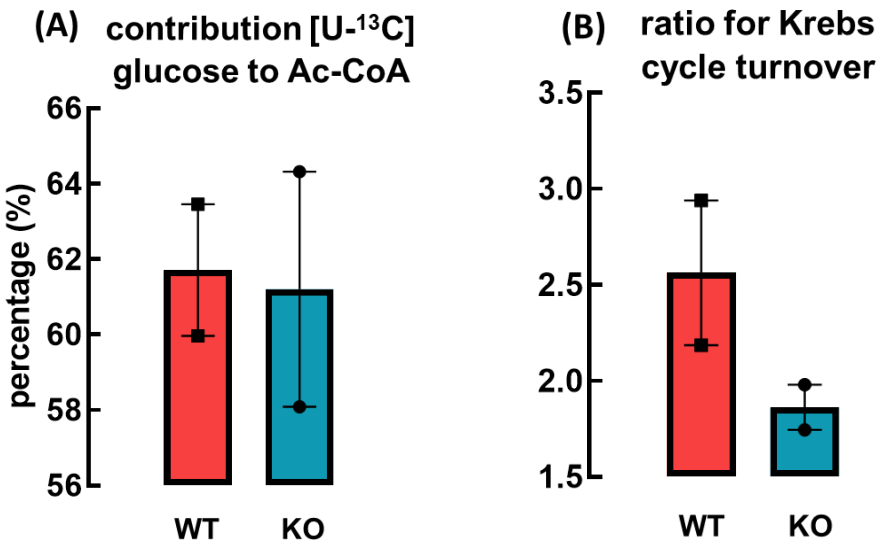

Figure 15: Metabolic parameters analysed through ^{13}C NMR spectra of cortical tissue extracts from male 3 months WT littermates and $A_{2A}R$ KO, pink and blue respectively. The parameters evaluated were: **(A)** contribution of [U-^{13}C]glucose to the enrichment of acetyl-CoA; **(B)** Ratio of Krebs cycle turnover. Student's unpaired *t* test. Data are presented as mean ± SEM and n=2 animals/group for all measured parameters. Student's unpaired *t* test.

5. Discussion

5.1. Protocol Optimization

Some experiments were performed in order to optimize the protocol. In this way, the first experiment aimed to select the optimal incubation time of metabolic substrates for incorporation into cerebrocortical synaptosomes. The time point selected was 7h, a limit imposed by the maximal viability of synaptosomes for a period up to 6-7h, as indicated by previous studies (94); at this time, we observed the highest peak intensities of the labelled lactate, which allowed us to assume that we were closer to a metabolic steady state, ideal for metabolic research (107).

Since the activity of nerve terminals could influence the metabolic profiling, we next compared resting and stimulated cerebrocortical synaptosomes. Thus, we assessed the effect of 4-aminopyridine (4-AP) in cerebrocortical synaptosomes purified from 9 months A_{2A}R KO male mice and WT littermates. 4-AP inhibits potassium channels leading to a threshold depolarization of synaptosomes, thus allowing intermittent burst-like neuronal activity (110). Some previous studies in rodents and humans concluded that neuronal activation induces different types of metabolic alterations: increased cerebral blood flow observed in rodent olfactory bulb (111); diminished the efficacy in the transport of nutrients, especially glucose, across the blood-brain barer (112); increased metabolic flow in the of Krebs cycle-associated amino acids, like glutamate and GABA, observed in rat hippocampal slices (109); and also a metabolic shift from almost a complete oxidation of glucose to an increased dependency on glycolysis, observed in humans (113).

Despite the results from these previous studies carried out in more integrated brain preparations, the present experiments performed in cerebrocortical synaptosomes showed no significant metabolic alterations in the presence compared to the absence of 4-AP. For this reason, we chose not to use 4-AP in the subsequent experiments.

5.2. Impact of aging on synaptic metabolism

Age-related studies were carried out using 3 months (young adults) and 9 months (adults) A_{2A}R KO mice and WT littermates. The reason for these experiments lies on the fact that

aging is one of the major risk factors related to neurodegenerative diseases, especially on the emergence cognitive and memory deficits (114).

With aging, the brain undergoes a series of metabolic changes: a gradual decline in energy utilization (115), probably arising from the glucose hypometabolism and mitochondrial dysfunction as also observed in humans (116–118); diminished blood-brain barer permeability, leading to a lower import of nutrients as observed in mice (119); and a decrease in the expression of glucose transporters as well as a change in the expression of key enzymes related to glycolysis and oxidative phosphorylation observed in humans (120). In relation to altered glycolytic enzymes, a study conducted in mice using ^{13}C and ^{1}H magnetic resonance spectroscopy (MRS), showed that the ratio between lactate dehydrogenase A and B (LDH A/LDH B) increases in older compared to young mice, leading to increased levels of lactate in aged mice (121).

In our studies, several alterations in the metabolic parameters evaluated were observed, revealing a change in the primary metabolism of cortical synapses upon aging, as concluded from the shift from oxidative to a more glycolytic metabolism. This would be in accordance with the previously mentioned study, although it must be kept in mind that the age of the older animals used in our study might not yet represent “aging” itself, as we compared animals considered young adults (3 months) and adults (9 months). In this way, and to further confirm and validate our conclusions, older mice (18/24 months) would be required to properly evaluate the alterations present in aged mice. Moreover, the results from the previous studies were all obtained using the whole brain or brain regions, rather than carried out specifically in nerve terminals as in our experiments.

5.3. Synapses in Alzheimer’s disease

Alzheimer’s disease (AD) is characterized by memory loss and dementia, starting with a progressive loss of synaptic function (24,27). Studies *in vivo* revealed bioenergetic alterations in patients with established AD features, such as a decrease in cerebral blood flow assessed by functional magnetic resonance imaging (fMRI), a decrease in glucose uptake monitored by positron emission tomography (PET) due to reduction in levels of GLUT1 and GLUT3 (20,56), and a reduced activity of some enzymes involved in the Krebs cycle and electron transport chain (122,123), that are consistent with a decrease in metabolic demand at the early stages of AD (124).

Glucose hypometabolism leads, through a decrease mitochondrial flux and respiratory function, to an impaired production of ATP (53), which can lead to synaptic dysfunction and neuronal death (125). In synapses, mitochondria play an essential role in maintaining the high energetic demand, although continuously generating reactive oxygen species (ROS), whose imbalance lead to oxidative stress, known to promote AD (51,52). Thus, oxidative stress associated with AD, originated from mitochondrial damage, can lead to decreased supply of energy to synapses and, as a result, to synaptic dysfunction (49,61,62).

Moreover, a link between lactate and AD has been proposed, based on the astrocyte-neuron lactate shuttle model (46,47), in which astrocytes metabolize glucose to lactate, which is released and taken up by nearby neurons and used as a fuel source. Aerobic glycolysis, where lactate is produced even in the presence of oxygen, is associated with neuroprotective roles in AD, as nerve cells resistant to Aβ display a metabolic shift towards an increased lactate production (126), a phenotype most common in cancer cells (127). Indeed, a study showed that the risk of developing AD is lower in cancer survivors than in people without cancer (128). However, more studies are needed on this subject to confirm this hypothesis (129).

Importantly, it is not known if the above mentioned metabolic modifications also occur in nerve terminals, that have particularly high metabolic demands (49). This question is particularly relevant to test the hypothesis that a metabolic dysfunction may be at the core of the synaptic dysfunction that is characteristic of early AD, as best heralded by the conclusion that AD is a synaptotoxicity at its onset (24). Thus, we now compared some key metabolic parameters in cerebrocortical synaptosomes prepared from WT mice and from APP/PS1 mice that model AD (86).

First, other colleagues within our group carried out a battery of behavioural tests to confirm that 6- and 9-months old APP/PS1 female mice and age–matched WT littermates displayed the key phenotypic traits of the early onset of AD, i.e. deficits of reference memory (29). Summarily, the results revealed that 6 months old APP/PS1 female mice had light memory impairments and anxiety, as assessed by the modified Y maze test and in the elevated plus maze test, respectively, and that 9 months old APP/PS1 female mice had learning and memory deficits and anxiety, monitored by the Morris water maze test and open field test (unpublished results), respectively.

The results presented in this thesis are not consistent with the hypothesis that metabolic deficits are prominent in cerebrocortical synapses at early AD, as they show no significant variations in synaptic metabolism between APP/PS1 mice and WT with 6 and 9 months.

In particular, experiments assessing the metabolism of synaptosomes, performed in APP/PS1 and WT with 6 months of age, showed no alterations in any of the metabolic parameters evaluated: [1,6-$^{13}C_2$]glucose consumption, [3-^{13}C]lactate production, and the percentages of glycolysis and OXPHOS. Moreover, in the substrate competition experiments in synaptosomes from 9 months old APP/PS1 and WT, only one of the three metabolic parameters assessed showed variations, [1,2-$^{13}C_2$] and [2-^{13}C]acetate production: the results revealed an increment of the production of [2-^{13}C]acetate compared to [1,2-$^{13}C_2$]acetate in APP/PS1 and WT, as well as an higher production of [2-^{13}C]acetate in APP/PS1 compared to WT, indicating that lactate is the apparent preferential substrate for the oxidative pathway.

The hypothesis posted when starting the present study was that early AD synaptic dysfunction would occur due to preceding metabolic alterations of synapses, providing that synapses are sensitive to bioenergetic changes owing to high energy demands (49). Despite not corroborating the hypothesis proposed, as no significant alterations in metabolic characteristics were observed, our results are in agreement with a previous study which revealed that in several transgenic mouse models of AD, no significant nor consistent deficits in bioenergetics were observed (130). Specifically, this study showed that synaptosomes from all the AD mice models exhibit normal respiratory variables, membrane potentials, mitochondrial volume fraction, and tolerance to calcium stress, apart from an increased respiration observed in APP/PS1 mice.

All these observations point out to a preservation of metabolic features in synaptosomes of the transgenic mouse model APP/PS1, a model of AD characterized by the appearance of Aβ deposits (29,86). Thus, based on our findings, there might be no gradual loss nor changes in the metabolic capacity of synapses associated with progressive synaptic dysfunction in early stages of AD.

However, it is worth noting that in the substrate competition experiment, lactate appeared to be the preferential substrate and that the production of acetate originated from labelled lactate was higher in female APP/PS1 mice than WT littermates. As mentioned before, Aβ resisting cells display a metabolic shift becoming more glycolytic (126), so a question rises of whether this apparent preservation of metabolic capacity of synapses, might be associated with aerobic glycolysis, meaning that lactate can act as a neuroprotector.

.

5.4. Neuroprotection: Caffeine and $A_{2A}R$ KO

Moderate caffeine intake affords neuroprotection against brain damage, especially related to cognitive and memory impairments, an effect likely involving $A_{2A}Rs$, since $A_{2A}R$ KO also display a decreased susceptibility to brain damage (16,92). However, the mechanisms by which caffeine is an important neuroprotective substance are still unknown (16). Since most neurodegenerative diseases are associated with oxidative stress and mitochondrial damage (37), the aim of these experiments was to test the hypothesis that caffeine and the genetic inactivation of $A_{2A}Rs$ might control primary metabolism as a mechanism to counteract any metabolic changes in the dysfunctional brain. This was investigated both in cerebrocortical synaptosomes and cortical slices: substrate competition experiments were performed in 3 months old WT male mice, half of which were administrated with caffeine, and 3 months old $A_{2A}R$ KO and WT male mice.

Caffeine metabolic impacts are yet not fully understood (16), but we know that the exposure to caffeine increases the rates of cerebral glucose utilization both upon acute and chronic consumption (68,69), although it also decreases cerebral blood flow (70). Duarte *et al* (71–73) showed, in hippocampal slices, that there were changes in the levels of taurine, which were increased in caffeine-treated mice. Moreover, in cellular models, caffeine is also known to ameliorate mitochondrial function, being an antioxidant substance (77–79).

The findings in synaptosomes of rats treated with caffeine indicated that there was an increase in [2-^{13}C]acetate production compared to [1,2-$^{13}C_2$]acetate production in both controls and caffeine-treated mice, leading to the assumption that lactate is the preferential substrate for the oxidative pathway in synaptosomes, since lactate produces higher amounts of acetate, meaning that it is being used the most for feeding the Krebs cycle, and therefore the oxidative pathway.

In cortical slices, which preserve most neuronal circuits and contain glial cells, we analysed metabolic alterations both in the medium and in tissue extracts, thus reflecting alterations of extracellular and intracellular metabolites, respectively. In the medium, there were no alterations in the levels of the analysed metabolites when comparing slices from animals exposed or not to caffeine. In the extracts, it was possible to take a closer look at what is happening in the Krebs cycle and thus the oxidative phosphorylation pathway. The results show that acetyl-CoA was generated at a higher percentage from [U-^{13}C]glucose compared to [3-^{13}C]lactate in slices from rats exposed to caffeine. Also, the results reveal a possible increase

in the contribution of [U-^{13}C]glucose in caffeine-treated mice compared to controls, although the number of samples is still too low (n=2) to establish firm conclusions. Nevertheless, the results lead us to assume that there might be no major differences in the primary metabolism of cerebrocortical synapses of mice subjected to chronic caffeine treatment.

To the best of our knowledge, no study has yet addressed possible metabolic alterations occurring in A_{2A}R KO mice, though a study performed in mice and focused on the heart, indicates that these animals had a significantly lower heart rate compared to WT mice, the locomotor activity was also lower in A_{2A}R KO compared to WT mice, and in male A_{2A}R KO mice compared to WT mice, the oxygen consumption was also decreased, with no alterations for female A_{2A}R KO (87).

The results of substrate competition experiments performed in A_{2A}R KO, revealed a decrease in [2-^{13}C]acetate production compared to [1,2-$^{13}C_2$]acetate production in both WT and A_{2A}R KO mice, contrasting with the caffeine results, and pointing out to glucose being the preferential energetic substrate in cortical A_{2A}R KO synaptosomes.

In relation to cortical slices, both media and tissue extracts were metabolically evaluated, thus distinguishing extracellular and intracellular metabolites, respectively. In medium samples, no alterations in the metabolic parameters evaluated were observed when comparing WT and A_{2A}R KO mice. In tissue extracts, it was possible to have more detailed information on the oxidative phosphorylation pathway. The results showed that acetyl-CoA was generated at a higher percentage from [U-^{13}C]glucose compared to [3-^{13}C]lactate, in the same way as for caffeine-treated mice experiments. Also, the Krebs cycle turnover from A_{2A}R KO mice was likely decreased compared to WT, although the number of samples is still too low (n=2), so no significant conclusion can be made. Nevertheless, the results lead us to assume that there might be no major differences in the primary metabolism of A_{2A}R KO mice.

Taking into consideration all the above described findings, we can infer that the caffeine- and A_{2A}R-related neuroprotective mechanisms may not have a significant association with metabolic alterations in normal mice, meaning that there is no metabolic compliance, even though we depicted small and distinct metabolic adaptations between both neuroprotective mechanisms.

Furthermore, in relation to the substrate competition, in synaptosomes, the results differ between caffeine treated mice, in which the preferential substrate is lactate, and A_{2A}R KO mice, in which glucose is the preferential substrate, whereas in slices, glucose is the preferential substrate for the oxidative phosphorylation pathway in both experimental conditions.

It is worth noting that in both experiments, a difference between the glycolytic index from synaptosomes (10x higher) and slices were observed, indicating that synaptosomes are, possibly, more glycolytic than slices. The reason for this can either be because the metabolism of synapses compared to the whole tissue is distinct, or due to the fact that there are two different biological preparations with distinct characteristics. One way to confirm whether different biological preparations can lead to different results, is to assess the mitochondrial respiratory capacity of both preparations and compare them.

In this way, the hypothesis that caffeine and the genetic inactivation of A_{2A}Rs might control primary metabolism as a mechanism to counteract any metabolic changes in the dysfunctional brain, was not supported by our findings.

6. Concluding remarks

The main goal of this research project was to evaluate the metabolic alterations underlying synaptic dysfunction in neurodegenerative diseases such as AD and understand whether metabolic adaptive changes in synapses could underlie neuroprotective processes (caffeine and selective $A_{2A}R$ blockade).

AD experiments revealed that there were no significant alterations in the metabolic parameters evaluated in cerebrocortical synapses. Since metabolic alteration are present in cortical region of patients with established AD, it is possible that the observed lack of metabolic alterations in cerebrocortical synapses might reflect a possible buffering of primary metabolism until the very limit of metabolic capacity in cortical synapses. Furthermore, unlike what was assumed, the preferential energy source in synaptosomes was lactate instead of glucose, so the hypothesis of a prominent role of aerobic glycolysis arises.

Moreover, our results show that the main source of energy in synaptosomes compared to slices is different, although the exact reasons for this difference remain unknown. A possibility is that there might be neurovascular deficits, leading to an impaired glucose transport, which could be assessed by evaluating the activity of GLUT in cerebrocortical synaptosomes.

In relation to neuroprotective processes, the experiments revealed that there are no alterations in the metabolism of synaptosomes or slices obtained from mice consuming caffeine daily compared to mice that do not consume caffeine at all. This apparently excludes adaptive metabolic changes as a possible mechanism of action of caffeine in the cerebral cortex and still leaves open the mechanisms underlying caffeine mediated neuroprotection.

All in all, these are just preliminary and general results, and several experiences should be performed next to confirm these results, and specially to uncover the questions and possibilities raised up by these experiments. Possible future experiments would be to use aged APP/PS1 mice and compare the same parameters to understand if there is a shift in the primary metabolism, or evaluate different metabolic parameters, pathways, and metabolites in relation to neuroprotective processes to assess if metabolic alterations arise.

7. References

1. Ackerman S. Discovering the Brain [Internet]. 1st ed. National Academy of Sciences, editor. Discovering the Brain. Washington, D.C.: National Academy Press; 1992. Available from: http://www.nap.edu/catalog/1785

2. Gooddy W, Reinhold M. The function of the cerebral cortex. Brain. 1954;77(3):416–26.

3. Stogsdill JA, Eroglu C. The interplay between neurons and glia in synapse development and plasticity. Curr Opin Neurobiol [Internet]. 2017;42:1–8. Available from: http://dx.doi.org/10.1016/j.conb.2016.09.016

4. Glasgow SD, McPhedrain R, Madranges JF, Kennedy TE, Ruthazer ES. Approaches and limitations in the investigation of synaptic transmission and plasticity. Front Synaptic Neurosci. 2019;11(JUL):1–16.

5. Domenici MR, Ferrante A, Martire A, Chiodi V, Pepponi R, Tebano MT, et al. Adenosine A2A receptor as potential therapeutic target in neuropsychiatric disorders. Pharmacol Res [Internet]. 2019;147(June):104338. Available from: https://doi.org/10.1016/j.phrs.2019.104338

6. Cunha RA. Adenosine as a neuromodulator and as a homeostatic regulator in the nervous system: Different roles, different sources and different receptors. Neurochem Int. 2001;38(2):107–25.

7. Haskó G, Antonioli L, Cronstein BN. Adenosine metabolism, immunity and joint health. Biochem Pharmacol [Internet]. 2018 May;151(12):307–13. Available from: https://linkinghub.elsevier.com/retrieve/pii/S0006295218300595

8. Borea PA, Gessi S, Merighi S, Vincenzi F, Varani K. Pharmacology of adenosine receptors: The state of the art. Physiol Rev. 2018;98(3):1591–625.

9. Fredholm BB, Chen J-F, Cunha RA, Svenningsson P, Vaugeois J-M. Adenosine and Brain Function. In 2005. p. 191–270. Available from: https://linkinghub.elsevier.com/retrieve/pii/S0074774205630073

10. Fastbom J, Pazos A, Palacios JM. The distribution of adenosine a1 receptors and 5'-nucleotidase in the brain of some commonly used experimental animals. Neuroscience. 1987;22(3):813–26.

11. Chen J-F, Eltzschig HK, Fredholm BB. Adenosine receptors as drug targets — what are the challenges? Nat Rev Drug Discov [Internet]. 2013 Apr 28;12(4):265–86. Available from: https://www.ncbi.nlm.nih.gov/pmc/articles/PMC3624763/pdf/nihms412728.pdf

12. Pagnussat N, Almeida AS, Marques DM, Nunes F, Chenet GC, Botton PHS, et al. Adenosine A2A receptors are necessary and sufficient to trigger memory impairment in adult mice. Br J Pharmacol. 2015;172(15):3831–45.

13. Rebola N, Canas PM, Oliveira CR, Cunha RA. Different synaptic and subsynaptic localization of adenosine A2A receptors in the hippocampus and striatum of the rat. Neuroscience. 2005;132(4):893–903.

14. Cunha RA. Neuroprotection by adenosine in the brain: From A1 receptor activation to A2A receptor blockade. Purinergic Signal. 2005;1(2):111–34.

15. Chen JF, Lee C fei, Chern Y. Adenosine receptor neurobiology: Overview [Internet]. 1st ed. Vol. 119, International Review of Neurobiology. Elsevier Inc.; 2014. 1–49 p. Available from: http://dx.doi.org/10.1016/B978-0-12-801022-8.00001-5

16. Cunha RA. How does adenosine control neuronal dysfunction and neurodegeneration? J Neurochem. 2016;139(6):1019–55.

17. Stockwell J, Jakova E, Cayabyab FS. Adenosine A1 and A2A receptors in the brain: Current research and their role in neurodegeneration. Molecules. 2017;22(4):1–18.

18. Angulo E, Casadó V, Mallol J, Canela EI, Viñals F, Ferrer I, et al. A1 Adenosine Receptors Accumulate in Neurodegenerative Structures in Alzheimer Disease and Mediate Both Amyloid Precursor Protein Processing and Tau Phosphorylation and Translocation. Brain Pathol. 2003;13(4):440–51.

19. Wang X, Zhou X, Li G, Zhang Y, Wu Y, Song W. Modifications and trafficking of APP in the pathogenesis of alzheimer's disease. Front Mol Neurosci. 2017;10(September):1–15.

20. Simpson IA, Chundu KR, Davies-Hill T, Honer WG, Davies P. Decreased concentrations of GLUT1 and GLUT3 glucose transporters in the brains of patients with Alzheimer's disease. Ann Neurol [Internet]. 1994 May;35(5):546–51. Available from: https://onlinelibrary.wiley.com/doi/10.1002/ana.410350507

21. Toledo JB, Arnold M, Kastenmüller G, Chang R, Baillie RA, Han X, et al. Metabolic network failures in Alzheimer's disease: A biochemical road map. Alzheimer's Dement [Internet]. 2017 Sep 21;13(9):965–84. Available from: https://onlinelibrary.wiley.com/doi/10.1016/j.jalz.2017.01.020

22. Seab JP, Jagust WJ, Wong STS, Roos MS, Reed BR, Budinger TF. Quantitative NMR measurements of hippocampal atrophy in Alzheimer's disease. Magn Reson Med.

1988;8(2):200–8.

23. Rusinek H, De Leon MJ, George AE, Stylopoulos LA, Chandra R, Smith G, et al. Alzheimer disease: Measuring loss of cerebral gray matter with MR imaging. Radiology. 1991;178(1):109–14.

24. Dennis J. Selkoe. Alzheimer's Disease Is a Synaptic Failure. Science (80-). 2002;298(5594):789–91.

25. Dong Y, Li X, Cheng J, Hou L. Drug development for alzheimer's disease: Microglia induced neuroinflammation as a target? Int J Mol Sci. 2019;20(3).

26. Scheff SW, Price DA. Alzheimer's disease-related alterations in synaptic density: Neocortex and hippocampus. J Alzheimer's Dis. 2006;9(SUPPL. 3):101–15.

27. Coleman P, Federoff H, Kurlan R. A focus on the synapse for neuroprotection in Alzheimer disease and other dementias. Neurology. 2004;63(7):1155–62.

28. Temido-Ferreira M, Ferreira DG, Batalha VL, Marques-Morgado I, Coelho JE, Pereira P, et al. Age-related shift in LTD is dependent on neuronal adenosine A2A receptors interplay with mGluR5 and NMDA receptors. Mol Psychiatry [Internet]. 2018;25(8):1876–900. Available from: http://dx.doi.org/10.1038/s41380-018-0110-9

29. Da Silva SV, Haberl MG, Zhang P, Bethge P, Lemos C, Gonçalves N, et al. Early synaptic deficits in the APP/PS1 mouse model of Alzheimer's disease involve neuronal adenosine A2A receptors. Nat Commun. 2016;7(May):1–11.

30. Kirby BY. Ad lib caffeine consumption, symptoms of caffeinism, and academic performance. Am J Psychiatry [Internet]. 1981 Apr;138(4):512–4. Available from: http://psychiatryonline.org/doi/abs/10.1176/ajp.138.4.512

31. Bertil B. Fredholm, Karl Bättig, Janet Holmén AN and EEZ. Actions of Caffeine in the Brain with Special Reference to Factors That Contribute to Its Widespread Use. Pharmacol Rev. 1999;51(1):83–133.

32. Lopes JP, Pliássova A, Cunha RA. The physiological effects of caffeine on synaptic transmission and plasticity in the mouse hippocampus selectively depend on adenosine A1 and A2A receptors. Biochem Pharmacol [Internet]. 2019;166(April):313–21. Available from: https://doi.org/10.1016/j.bcp.2019.06.008

33. Chen JF. Adenosine receptor control of cognition in normal and disease [Internet]. 1st

ed. Vol. 119, International Review of Neurobiology. Elsevier Inc.; 2014. 257–307 p. Available from: http://dx.doi.org/10.1016/B978-0-12-801022-8.00012-X

34. Cunha RA, Agostinho PM. Chronic caffeine consumption prevents memory disturbance in different animal models of memory decline. J Alzheimer's Dis. 2010;20(SUPPL.1).

35. D'Alcantara P, Ledent C, Swillens S, Schiffmann SN. Inactivation of adenosine A2A receptor impairs long term potentiation in the accumbens nucleus without altering basal synaptic transmission. Neuroscience. 2001;107(3):455–64.

36. Salmi P, Chergui K, Fredholm BB. Adenosine-dopamine interactions revealed in knockout mice. J Mol Neurosci. 2005;26(2–3):239–44.

37. Camandola S, Mattson MP. Brain metabolism in health, aging, and neurodegeneration. EMBO J. 2017;36(11):1474–92.

38. Mergenthaler P, Lindauer U, Dienel GA, Meisel A. Sugar for the brain: The role of glucose in physiological and pathological brain function. Trends Neurosci. 2013;36(10):587–97.

39. Steele ML, Robinson SR. Reactive astrocytes give neurons less support: Implications for Alzheimer's disease. Neurobiol Aging [Internet]. 2012;33(2):423.e1-423.e13. Available from: http://dx.doi.org/10.1016/j.neurobiolaging.2010.09.018

40. Hertz L, Dienel GA. Energy metabolism in the brain. In: International Review of Neurobiology [Internet]. 2002. p. 1-IN4. Available from: https://linkinghub.elsevier.com/retrieve/pii/S0074774202510035

41. Martínez-Reyes I, Chandel NS. Mitochondrial TCA cycle metabolites control physiology and disease. Nat Commun [Internet]. 2020;11(1):1–11. Available from: http://dx.doi.org/10.1038/s41467-019-13668-3

42. Figley CR, Stroman PW. The role(s) of astrocytes and astrocyte activity in neurometabolism, neurovascular coupling, and the production of functional neuroimaging signals. Eur J Neurosci. 2011;33(4):577–88.

43. Laughton JD, Charnay Y, Belloir B, Pellerin L, Magistretti PJ, Bouras C. Differential messenger RNA distribution of lactate dehydrogenase LDH-1 and LDH-5 isoforms in the rat brain. Neuroscience. 2000;96(3):619–25.

44. Pellerin L, Magistretti PJ. Food for Thought: Challenging the Dogmas. J Cereb Blood Flow Metab. 2003;23(11):1282–6.

45. Loaiza A, Porras OH, Barros LF. Glutamate triggers rapid glucose transport stimulation in astrocytes as evidenced by real-time confocal microscopy. J Neurosci. 2003;23(19):7337–42.

46. Pellerin L, Bouzier-Sore A-K, Aubert A, Serres S, Merle M, Costalat R, et al. Activity-dependent regulation of energy metabolism by astrocytes: An update. Glia [Internet]. 2007 Sep;55(12):1251–62. Available from: http://www.unscn.org/en/home/

47. Allaman I, Bélanger M, Magistretti PJ. Astrocyte-neuron metabolic relationships: For better and for worse. Trends Neurosci. 2011;34(2):76–87.

48. Mason S. Lactate shuttles in neuroenergetics-homeostasis, allostasis and beyond. Front Neurosci. 2017;11(FEB):1–15.

49. Harris JJ, Jolivet R, Attwell D. Synaptic Energy Use and Supply. Neuron. 2012;75(5):762–77.

50. Wyss MT, Jolivet R, Buck A, Magistretti PJ, Weber B. In Vivo evidence for lactate as a neuronal energy source. J Neurosci. 2011;31(20):7477–85.

51. Hensley K, Hall N, Subramaniam R, Cole P, Harris M, Aksenov M, et al. Brain Regional Correspondence Between Alzheimer's Disease Histopathology and Biomarkers of Protein Oxidation. J Neurochem. 1995;65(5):2146–56.

52. Cheignon C, Tomas M, Bonnefont-Rousselot D, Faller P, Hureau C, Collin F. Oxidative stress and the amyloid beta peptide in Alzheimer's disease. Redox Biol [Internet]. 2018;14(October 2017):450–64. Available from: http://dx.doi.org/10.1016/j.redox.2017.10.014

53. Allan Butterfield D, Boyd-Kimball D. Oxidative Stress, Amyloid-β Peptide, and Altered Key Molecular Pathways in the Pathogenesis and Progression of Alzheimer's Disease. J Alzheimer's Dis. 2018;62(3):1345–67.

54. Sultana R, Reed T, Perluigi M, Coccia R, Pierce WM, Butterfield DA. Proteomic identification of nitrated brain proteins in amnestic mild cognitive impairment: A regional study. J Cell Mol Med. 2007;11(4):839–51.

55. Di Domenico F, Barone E, Perluigi M, Butterfield DA. The Triangle of Death in Alzheimer's Disease Brain: The Aberrant Cross-Talk among Energy Metabolism, Mammalian Target of Rapamycin Signaling, and Protein Homeostasis Revealed by Redox Proteomics. Antioxidants Redox Signal. 2017;26(8):364–87.

56. Landau SM, Harvey D, Madison CM, Reiman EM, Foster NL, Aisen PS, et al. Comparing predictors of conversion and decline in mild cognitive impairment. Neurology. 2010;75(3):230–8.

57. Iwangoff P, Armbruster R, Enz A, Meier-Ruge W. Glycolytic enzymes from human autoptic brain cortex: Normal aged and demented cases. Mech Ageing Dev [Internet]. 1980 Sep;14(1–2):203–9. Available from: https://linkinghub.elsevier.com/retrieve/pii/0047637480901207

58. Perry EK, Perry RH, Tomlinson BE, Blessed G, Gibson PH. Coenzyme a-acetylating enzymes in Alzheimer's disease: Possible cholinergic "compartment" of pyruvate dehydrogenase. Neurosci Lett. 1980;18(1):105–10.

59. Rui Y, Tiwari P, Xie Z, Zheng JQ. Acute impairment of mitochondrial trafficking by β-amyloid peptides in hippocampal neurons. J Neurosci. 2006;26(41):10480–7.

60. Shahpasand K, Uemura I, Saito T, Asano T, Hata K, Shibata K, et al. Regulation of mitochondrial transport and inter-microtubule spacing by tau phosphorylation at the sites hyperphosphorylated in Alzheimer's disease. J Neurosci. 2012;32(7):2430–41.

61. Reddy PH, Manczak M, Mao P, Calkins MJ, Reddy AP, Shirendeb U. Amyloid-β and mitochondria in aging and Alzheimer's disease: Implications for synaptic damage and cognitive decline. J Alzheimer's Dis. 2010;20(SUPPL.2).

62. Eckert A, Schmitt K, Götz J. Mitochondrial dysfunction - The beginning of the end in Alzheimer's disease? Separate and synergistic modes of tau and amyloid-toxicity. Alzheimer's Res Ther. 2011;3(3).

63. Rogers NL, Dinges DF. Caffeine: Implications for alertness in athletes. Clin Sports Med. 2005;24(2):1–13.

64. Aguiar AS, Speck AE, Canas PM, Cunha RA. Neuronal adenosine A2A receptors signal ergogenic effects of caffeine. Sci Rep [Internet]. 2020;10(1):1–10. Available from: https://doi.org/10.1038/s41598-020-69660-1

65. Ahrendt DM. Ergogenic aids: Counseling the athlete. Am Fam Physician. 2001;63(5):913–22.

66. Canas PM, Porciúncula LO, Cunha GMA, Silva CG, Machado NJ, Oliveira JMA, et al. Adenosine A2A receptor blockade prevents synaptotoxicity and memory dysfunction caused by β-amyloid peptides via p38 mitogen-activated protein kinase pathway. J

Neurosci. 2009;29(47):14741–51.

67. Arendash GW, Schleif W, Rezai-Zadeh K, Jackson EK, Zacharia LC, Cracchiolo JR, et al. Caffeine protects Alzheimer's mice against cognitive impairment and reduces brain β-amyloid production. Neuroscience. 2006;142(4):941–52.

68. Nehlig A, de Vasconcelos AP, Collignon A, Boyet S. Comparative effects of caffeine and L-phenylisopropyladenosine on local cerebral glucose utilization in the rat. Eur J Pharmacol. 1988;157(1):1–11.

69. Nehlig A, Daval JL, Debry G. Caffeine and the central nervous system: mechanisms of action. Brain Res Rev. 1992;17(2):139–70.

70. Nehlig A, Pereira De Vasconcelos A, Boyet S. Effects of caffeine and/or l-phenylisopropyladenosine (lpia) on local cerebral blood flow and glucose utilization in the rat. Nucleosides and Nucleotides. 1991;10(5):1225–6.

71. Duarte JMN, Carvalho RA, Cunha RA, Gruetter R. Caffeine consumption attenuates neurochemical modifications in the hippocampus of streptozotocin-induced diabetic rats. J Neurochem. 2009;111(2):368–79.

72. Duarte JMN, Agostinho PM, Carvalho RA, Cunha RA. Caffeine consumption prevents diabetes-induced memory impairment and synaptotoxicity in the hippocampus of nonczno10/ltj mice. PLoS One. 2012;7(4):1–10.

73. Duarte JMN, Skoug C, Silva HB, Carvalho RA, Gruetter R, Cunha RA. Impact of caffeine consumption on type 2 diabetes-induced spatial memory impairment and neurochemical alterations in the hippocampus. Front Neurosci. 2019;13(JAN).

74. Pasantes-Morales H. Taurine homeostasis and volume control. Adv Neurobiol. 2017;16(mM):33–53.

75. Hansen SH, Andersen ML, Cornett C, Gradinaru R, Grunnet N. A role for taurine in mitochondrial function. J Biomed Sci. 2010;17(SUPPL. 1):1–8.

76. Hada J, Kaku T, Morimoto K, Hayashi Y, Nagai K. Activation of adenosine A2 receptors enhances high K+-evoked taurine release from rat hippocampus: A microdialysis study. Amino Acids [Internet]. 1998 Mar;15(1–2):43–52. Available from: http://link.springer.com/10.1007/BF01345279

77. Samadi M, Shaki F, Bameri B, Fallah M, Ahangar N, Mohammadi H. Caffeine attenuates

seizure and brain mitochondrial disruption induced by Tramadol: the role of adenosinergic pathway. Drug Chem Toxicol [Internet]. 2021;44(6):613–9. Available from: https://doi.org/10.1080/01480545.2019.1643874

78. Devasagayam TPA, Kamat JP, Mohan H, Kesavan PC. Caffeine as an antioxidant: inhibition of lipid peroxidation induced by reactive oxygen species. Biochim Biophys Acta - Biomembr [Internet]. 1996 Jun;1282(1):63–70. Available from: https://linkinghub.elsevier.com/retrieve/pii/0005273696000405

79. Mishra J, Kumar A. Improvement of mitochondrial NAD+/FAD+-linked state-3 respiration by caffeine attenuates quinolinic acid induced motor impairment in rats: Implications in Huntington's disease. Pharmacol Reports [Internet]. 2014;66(6):1148–55. Available from: http://dx.doi.org/10.1016/j.pharep.2014.07.006

80. Souza MA, Mota BC, Gerbatin RR, Rodrigues FS, Castro M, Fighera MR, et al. Antioxidant activity elicited by low dose of caffeine attenuates pentylenetetrazol-induced seizures and oxidative damage in rats. Neurochem Int [Internet]. 2013;62(6):821–30. Available from: http://dx.doi.org/10.1016/j.neuint.2013.02.021

81. Aoyama K, Matsumura N, Watabe M, Wang F, Kikuchi-Utsumi K, Nakaki T. Caffeine and uric acid mediate glutathione synthesis for neuroprotection. Neuroscience [Internet]. 2011;181:206–15. Available from: http://dx.doi.org/10.1016/j.neuroscience.2011.02.047

82. Canas PM, Duarte JMN, Rodrigues RJ, Köfalvi A, Cunha RA. Modification upon aging of the density of presynaptic modulation systems in the hippocampus. Neurobiol Aging. 2009;30(11):1877–84.

83. Matos M, Augusto E, MacHado NJ, Dos Santos-Rodrigues A, Cunha RA, Agostinho P. Astrocytic adenosine A2A receptors control the amyloid-β peptide-induced decrease of glutamate uptake. J Alzheimer's Dis. 2012;31(3):555–67.

84. Mohamed RA, Agha AM, Abdel-Rahman AA, Nassar NN. Role of adenosine A2A receptor in cerebral ischemia reperfusion injury: Signaling to phosphorylated extracellular signal-regulated protein kinase (pERK1/2). Neuroscience [Internet]. 2016;314(December):145–59. Available from: http://dx.doi.org/10.1016/j.neuroscience.2015.11.059

85. Lopes CR, Lourenço VS, Tomé ÂR, Cunha RA, Canas PM. Use of knockout mice to explore CNS effects of adenosine. Biochem Pharmacol. 2021;187(December).

86. Jankowsky JL, Fadale DJ, Anderson J, Xu GM, Gonzales V, Jenkins NA, et al. Mutant presenilins specifically elevate the levels of the 42 residue β-amyloid peptide in vivo: Evidence for augmentation of a 42-specific γ secretase. Hum Mol Genet. 2004;13(2):159–70.

87. Yang JN, Chen JF, Fredholm BB. Physiological roles of A 1 and A 2A adenosine receptors in regulating heart rate, body temperature, and locomotion as revealed using knockout mice and caffeine. Am J Physiol - Hear Circ Physiol. 2009;296(4).

88. Simões-Henriques C, Mateus-Pinheiro M, Gaspar R, Pinheiro H, Mendes Duarte J, Baptista FI, et al. Microglia cytoarchitecture in the brain of adenosine A2A receptor knockout mice: Brain region and sex specificities. Eur J Neurosci. 2020;51(6):1377–87.

89. Troncoso F, Herlitz K, Acurio J, Aguayo C, Guevara K, Castro FO, et al. Advantages in wound healing process in female mice require upregulation A2A-mediated angiogenesis under the stimulation of 17β-estradiol. Int J Mol Sci. 2020;21(19):1–18.

90. Huang QY, Wei C, Yu L, Coelho JE, Shen HY, Kalda A, et al. Adenosine A2A receptors in bone marrow-derived cells but not in forebrain neurons are important contributors to 3-nitropropionic acid-induced striatal damage as revealed by cell-type-selective inactivation. J Neurosci. 2006;26(44):11371–8.

91. Yu L, Huang Z, Mariani J, Wang Y, Moskowitz M, Chen JF. Selective inactivation or reconstitution of adenosine A2A receptors in bone marrow cells reveals their significant contribution to the development of ischemic brain injury. Nat Med. 2004;10(10):1081–7.

92. Chen JF, Huang Z, Ma J, Zhu JM, Moratalla R, Standaert D, et al. A(2A) adenosine receptor deficiency attenuates brain injury induced by transient focal ischemia in mice. J Neurosci. 1999;19(21):9192–200.

93. Rodrigues RJ, Marques JM, Cunha RA. Purinergic signalling and brain development. Semin Cell Dev Biol [Internet]. 2019;95(August):34–41. Available from: https://doi.org/10.1016/j.semcdb.2018.12.001

94. Raiteri M, Angelini F, Levi G. A simple apparatus for studying the release of neurotransmitters from synaptosomes. Eur J Pharmacol. 1974;25(3):411–4.

95. Cunha RA, Sebastião AM, Ribeiro JA. Inhibition by ATP of hippocampal synaptic transmission requires localized extracellular catabolism by ecto-nucleotidases into

adenosine and channeling to adenosine A1 receptors. J Neurosci. 1998;18(6):1987–95.

96. Moreira-de-Sá A, Gonçalves FQ, Lopes JP, Silva HB, Tomé ÂR, Cunha RA, et al. Adenosine A2A receptors format long-term depression and memory strategies in a mouse model of Angelman syndrome. Neurobiol Dis [Internet]. 2020;146(October):105137. Available from: https://doi.org/10.1016/j.nbd.2020.105137

97. Dunkley PR, Jarvie PE, Robinson PJ. A rapid Percoll gradient procedure for preparation of synaptosomes. Nat Protoc [Internet]. 2008 Nov 16;3(11):1718–28. Available from: http://www.nature.com/articles/nprot.2008.171

98. Canas PM, Cunha RA. Subsynaptic Membrane Fractionation. In: Neuromethods [Internet]. 2021. p. 31–8. Available from: https://link.springer.com/10.1007/978-1-0716-1522-5_3

99. Lin CY, Wu H, Tjeerdema RS, Viant MR. Evaluation of metabolite extraction strategies from tissue samples using NMR metabolomics. Metabolomics. 2007;3(1):55–67.

100. Beckonert O, Keun HC, Ebbels TMD, Bundy J, Holmes E, Lindon JC, et al. Metabolic profiling, metabolomic and metabonomic procedures for NMR spectroscopy of urine, plasma, serum and tissue extracts. Nat Protoc. 2007;2(11):2692–703.

101. Yamamoto C, McIlwain H. Electrical Activities in Thin Sections From the Mammalian Brain Maintained in Chemically-Defined Media in Vitro. J Neurochem. 1966;13(12):1333–43.

102. McNair LF, Kornfelt R, Walls AB, Andersen J V., Aldana BI, Nissen JD, et al. Metabolic Characterization of Acutely Isolated Hippocampal and Cerebral Cortical Slices Using [U-13C]Glucose and [1,2-13C]Acetate as Substrates. Neurochem Res. 2017;42(3):810–26.

103. Fredholm BB, Dunwiddie T V., Bergman B, Lindström K. Levels of adenosine and adenine nucleotides in slices of rat hippocampus. Brain Res. 1984;295(1):127–36.

104. Crook AA, Powers R. Quantitative NMR-Based Biomedical Metabolomics: Current Status and Applications. Molecules. 2020;25(21).

105. Glickson JD, Opella SJ. Carbon-13 NMR spectroscopy of biological systems. Vol. 10, Concepts in Magnetic Resonance. 1998. 129–130 p.

106. Markley JL, Brüschweiler R, Edison AS, Eghbalnia HR, Powers R, Raftery D, et al. The future of NMR-based metabolomics. Curr Opin Biotechnol [Internet]. 2017 Feb;43(5):34–40. Available from: https://linkinghub.elsevier.com/retrieve/pii/S0958166916301768

107. Reijngoud DJ. Flux analysis of inborn errors of metabolism. J Inherit Metab Dis. 2018;41(3):309–28.

108. Tibbs GR, Barrie AP, Van Mieghem FJE, McMahon HT, Nicholls DG. Repetitive Action Potentials in Isolated Nerve Terminals in the Presence of 4-Aminopyridine: Effects on Cytosolic Free Ca2+ and Glutamate Release. J Neurochem. 1989;53(6):1693–9.

109. Duarte JMN, Cunha RA, Carvalho RA. Different metabolism of glutamatergic and GABAergic compartments in superfused hippocampal slices characterized by nuclear magnetic resonance spectroscopy. Neuroscience. 2007;144(4):1305–13.

110. Tapia R, Sitges M. Effect of 4-aminopyridine on transmitter release in synaptosomes. Brain Res. 1982;250(2):291–9.

111. Chaigneau E, Tiret P, Lecoq J, Ducros M, Knöpfel T, Charpak S. The relationship between blood flow and neuronal activity in the rodent olfactory bulb. J Neurosci. 2007;27(24):6452–60.

112. Leybaert L. Neurobarrier coupling in the brain: A partner of neurovascular and neurometabolic coupling? J Cereb Blood Flow Metab. 2005;25(1):2–16.

113. Fox PT, Raichle ME, Mintun MA, Dence C. Nonoxidative glucose consumption during focal physiologic neural activity. Science (80-). 1988;241(4864):462–4.

114. Bettio LEB, Rajendran L, Gil-Mohapel J. The effects of aging in the hippocampus and cognitive decline. Neurosci Biobehav Rev [Internet]. 2017;79:66–86. Available from: http://dx.doi.org/10.1016/j.neubiorev.2017.04.030

115. Hoyer S. The young-adult and normally aged brain. Its blood flow and oxidative metabolism. A review - part I. Arch Gerontol Geriatr. 1982;1(2):101–16.

116. Mosconi L, De Santi S, Li J, Tsui WH, Li Y, Boppana M, et al. Hippocampal hypometabolism predicts cognitive decline from normal aging. Neurobiol Aging [Internet]. 2008 May;29(5):676–92. Available from: https://linkinghub.elsevier.com/retrieve/pii/S0197458006004611

117. Small GW, Ercoli LM, Silverman DHS, Huang SC, Komo S, Bookheimer SY, et al. Cerebral metabolic and cognitive decline in persons at genetic risk for Alzheimer's disease. Proc Natl Acad Sci U S A. 2000;97(11):6037–42.

118. de Leon MJ, Ferris SH, George AE, Reisberg B, Christman DR, Kricheff II, et al. Computed

tomography and positron emission transaxial tomography evaluations of normal aging and Alzheimer's disease. J Cereb Blood Flow Metab. 1983;3(3):391–4.

119. Winkler EA, Nishida Y, Sagare AP, Rege S V, Bell RD, Perlmutter D, et al. GLUT1 reductions exacerbate Alzheimer's disease vasculo-neuronal dysfunction and degeneration. Nat Neurosci [Internet]. 2015 Apr 2;18(4):521–30. Available from: http://www.nature.com/articles/nn.3966

120. Meier-Ruge W, Iwangoff P, Reichlmeier K, Sandoz P. Neurochemical findings in the aging brain. Adv Biochem Psychopharmacol [Internet]. 1980;23:323–38. Available from: http://www.ncbi.nlm.nih.gov/pubmed/6446847

121. Ross JM, Öberg J, Brené S, Coppotelli G, Terzioglu M, Pernold K, et al. High brain lactate is a hallmark of aging and caused by a shift in the lactate dehydrogenase A/B ratio. Proc Natl Acad Sci U S A. 2010;107(46):20087–92.

122. Liang WS, Reiman EM, Valla J, Dunckley T, Beach TG, Grover A, et al. Alzheimer's disease is associated with reduced expression of energy metabolism genes in posterior cingulate neurons. Proc Natl Acad Sci U S A. 2008;105(11):4441–6.

123. Brooks WM, Lynch PJ, Ingle CC, Hatton A, Emson PC, Faull RLM, et al. Gene expression profiles of metabolic enzyme transcripts in Alzheimer's disease. Brain Res. 2007;1127(1):127–35.

124. Chandrasekaran K, Hatanpää K, Brady DR, Rapoport SI. Evidence for physiological down-regulation of brain oxidative phosphorylation in Alzheimer's disease. Exp Neurol. 1996;142(1):80–8.

125. Caughey B, Lansbury PT. Protofibrils, pores, fibrils, and neurodegeneration: Separating the responsible protein aggregates from the innocent bystanders. Annu Rev Neurosci. 2003;26:267–98.

126. Newington JT, Pitts A, Chien A, Arseneault R, Schubert D, Cumming RC. Amyloid beta resistance in nerve cell lines is mediated by the warburg effect. PLoS One. 2011;6(4).

127. Burke RE, Harris SC, McGuire WL. Lactate Dehydrogenase in Estrogen-responsive Human Breast Cancer Cells. Cancer Res. 1978;38(9):2773–6.

128. Driver JA, Beiser A, Au R, Kreger BE, Splansky GL, Kurth T, et al. Inverse association between cancer and Alzheimer's disease: Results from the Framingham Heart Study. BMJ. 2012;344(7850):19.

129. Newington JT, Harris RA, Cumming RC. Reevaluating Metabolism in Alzheimer's Disease from the Perspective of the Astrocyte-Neuron Lactate Shuttle Model. J Neurodegener Dis. 2013;2013:1–13.

130. Choi SW, Gerencser AA, Ng R, Flynn JM, Melov S, Danielson SR, et al. No consistent bioenergetic defects in presynaptic nerve terminals isolated from mouse models of Alzheimer's disease. J Neurosci. 2012;32(47):16775–84.